Supplementary Information

Multistimuli-Responsive and Multimode Azoquinoline Chiroptical Switches

Zimu Liu,[a,b] Youming Lv,[a,c*] Hebo Ye,[a*] Hanwei Lu,[a] and Lei You[a,c,d*]

[a]State Key Laboratory of Structural Chemistry, Fujian Institute of Research on the Structure of Matter, Chinese Academy of Sciences, Fuzhou 350002, China.

[b]College of Chemistry and Material Science, Fujian Normal University, Fuzhou 350007, China.

[c]University of Chinese Academy of Sciences, Beijing 100049,

[d]Fujian Science & Technology Innovation Laboratory for Optoelectronic Information of China, Fuzhou 350108, China.

TABLE OF CONTENTS

1. General methods

^{1}H NMR spectra were recorded on a 400 MHz Bruker Biospin avance III spectrometer. Deuterated reagents for characterization and *in situ* reactions were purchased from Sigma-Aldrich Chemical Co. and Cambridge Isotope Laboratories, Inc. (purity ≥ 99.9%). All other reagents were obtained from commercial sources and used without further purification, unless indicated otherwise. The chemical shifts (δ) for ^{1}H NMR spectra, given in ppm, are referenced to the residual proton signal of the deuterated solvent. Mass spectra were recorded on a Bruker IMPACT-II or ThermoScientificLCQ Fleet spectrometer. Crystallographic data was collected on a Mercury single crystal diffractometer. The structures were solved with direct methods by using OlexSys or SHELXS-97 and refined with the full-matrix least-squares technique based on F2. The UV-vis spectra were recorded on a Shimadzu UV-1900i spectrometer.

Dynamic covalent reactions. Dynamic covalent reactions (DCRs) were performed *in situ* in DMSO-d_6 at room temperature without isolation and purification. The mixture was characterized by ^{1}H NMR and mass spectroscopy (MS). See specific conditions in figure captions of the main text or supplementary information if necessary.

Irradiation experiments. The UV and Visible light irradiation experiments were carried out on a UV LED strip light (wavelength = 365 nm, power = 20 W) and a blue LED strip light (wavelength = 425 nm, power = 20 W), respectively.

Determination of thermal half-lives. Each azoarene (at a concentration of 10 mM) in DMSO-d_6 was irradiated with a 365 nm LED for at least 1.5 h to produce *Z* isomer, and then placed in a dark environment at a constant temperature (25 ºC). ^{1}H NMR spectra were used to monitor the thermal conversion of azoarene from *Z* to *E* isomer. Each azoarene in $CHCl_3$ (at a concentration of 0.10 mM) was irradiated with a 365 nm LED for 2 min to produce the *Z* isomer, and then placed in a dark environment at a constant temperature (25 °C). UV-vis spectra were used to monitor the thermal conversion of azoarene from *Z* to *E* isomer. Rate constants (k) for the first order thermal isomerization were determined from exponential fit of a graph of percent of *Z* isomer vs. time, where $t_{½} = \ln(2)/k$.[S1]

Circular dichroism (CD) spectroscopy. Circular dichroism (CD) spectroscopy was measured in a chloroform solution at room temperature. After the dynamic covalent reactions of *E*-**1** (10 mM), one primary amine (1.5 equiv.), and one metal salt (1.2 equiv.) in DMSO was complete, the reaction mixture was diluted to 0.10 mM with chloroform, and CD spectra were then recorded on a BioLogic MOS-450 spectropolarimeter. For CD titrations, the solutions of imines or their complexes were prepared as described followed by the addition of the metal salt.

DFT Calculations. Geometry optimization and frequencies calculations were performed by using Gaussian 09 (G09) packages,[S2] with the DFT method and basis set of B3LYP-D3(BJ)/def2-SVP. The PCM model of DMSO and the ultrafine integration grid were also employed. All the geometries were determined without imaginary frequencies by frequency analysis. With the same settings, the time-dependent DFT calculation of electronic circular dichroism (ECD) and UV-vis spectra was conducted. CD spectra were generated by using Multiwfn 3.8[S3] with gaussian band shape of 0.333 eV exponential half-width from velocity representation. The visualization of the orbitals was presented by VMD 1.90[S4].

E-**1** was synthesized and purified according to the literature.[S5] ^{1}H NMR (400 MHz, 20 °C, DMSO-d_6): δ = 9.10 (d, *J* = 5.3 Hz, 1H), 8.55 (d, *J* = 8.3 Hz, 1H), 8.42-8.16 (m, *J* = 12.1, 8.8 Hz, 2H), 8.11-7.85 (m, 2H), 7.85-7.57 (m, 4H), 6.77 (br, 1H). ^{13}C NMR (101 MHz, 20 °C, DMSO-d_6) δ = 151.7, 149.6, 148.8, 143.6, 136.5, 132.30, 128.8, 126.6, 122.5, 116.3. ESI-HRMS: *m/z* calculated for $C_{17}H_{12}N_3O_3$ $[M + H]^+$: 306.0873; found: 306.0878.

2. Synergistic effects of chiral amines with metal ions

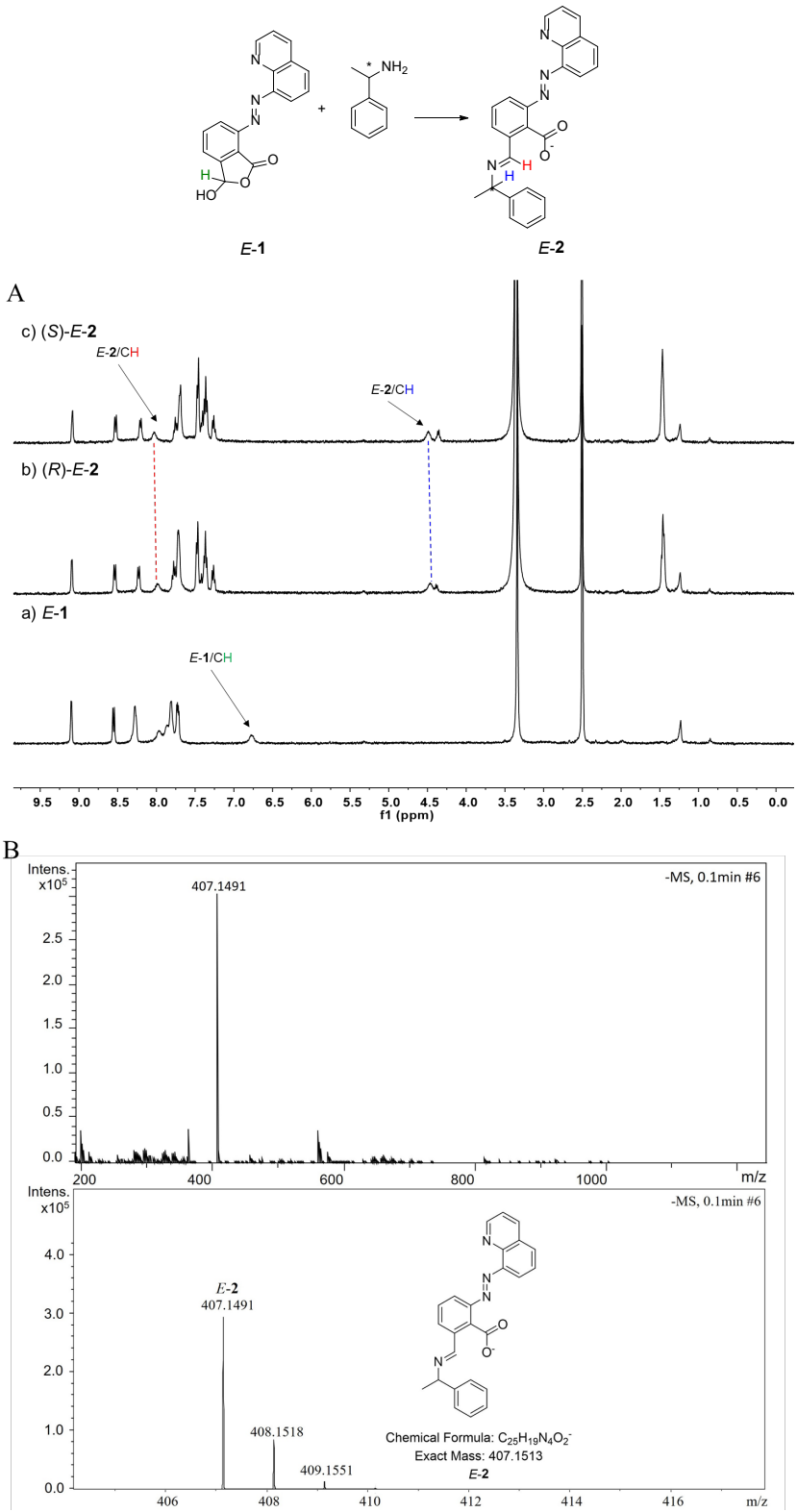

Figure S1. (A) (a) ^{1}H NMR (400 MHz, 20 °C) spectrum of *E*-**1** (10 mM) in DMSO-d_6; (b) After addition of 1.5 equiv. of (*R*)-1-phenylethylamine (b) and (*S*)-1-phenylethylamine (c) into panel a. The reactions reached equilibrium within 15 min. (B) MS spectra of *E*-**2**.

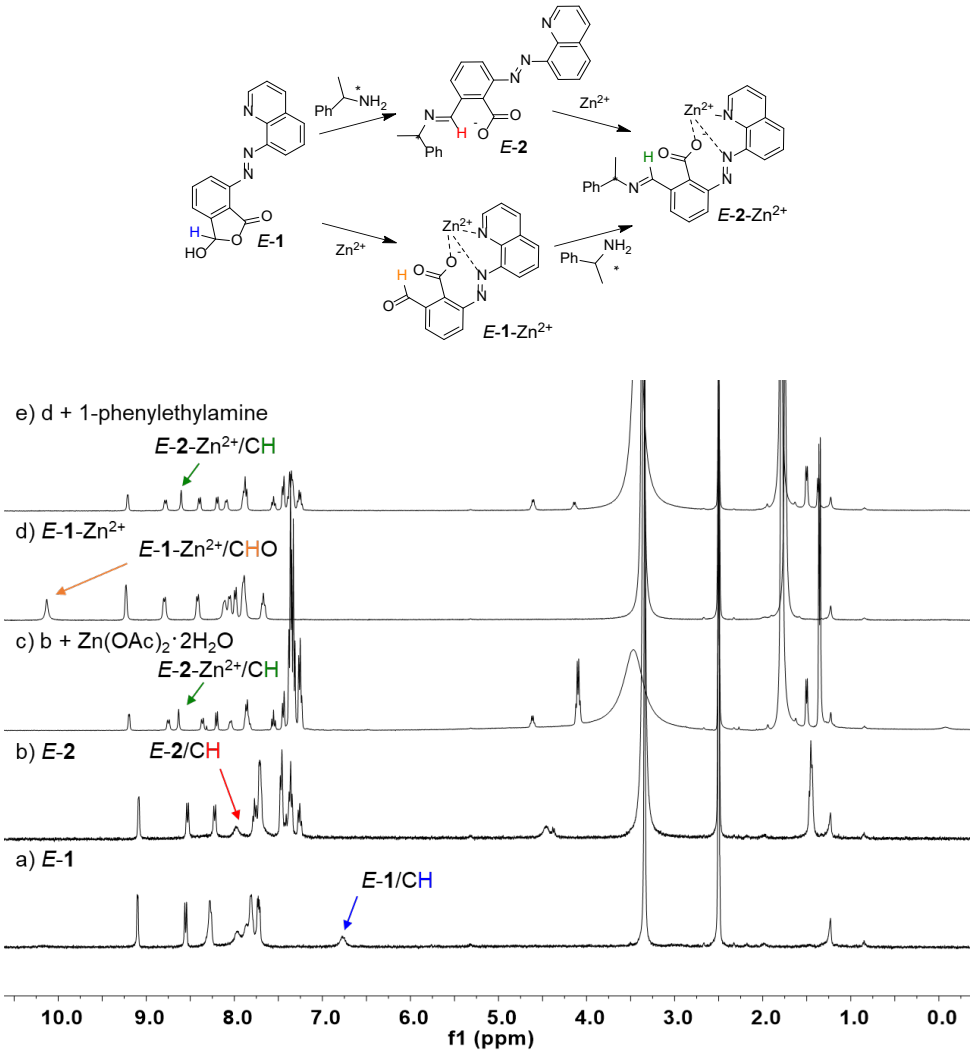

Figure S2. ^{1}H NMR (400 MHz, 20 °C) spectra of *E*-**1** (10 mM) (a) and *E*-**2** (10 mM, created *in situ* from the reaction of *E*-**1** and (*R*)-1-phenylethylamine (1.5 equiv.) in DMSO-d_6) (b). After addition of 1.2 equiv. $Zn(OAc)_2{\cdot}2H_2O$ into panel b (c). *E*-**1**-Zn^{2+}(10 mM, created *in situ* from the addition of 1.2 equiv. $Zn(OAc)_2{\cdot}2H_2O$ into *E*-**1** in DMSO-d_6) (d) and further addition of 1.5 equiv. of (*R*)-1-phenylethylamine into panel d (e).

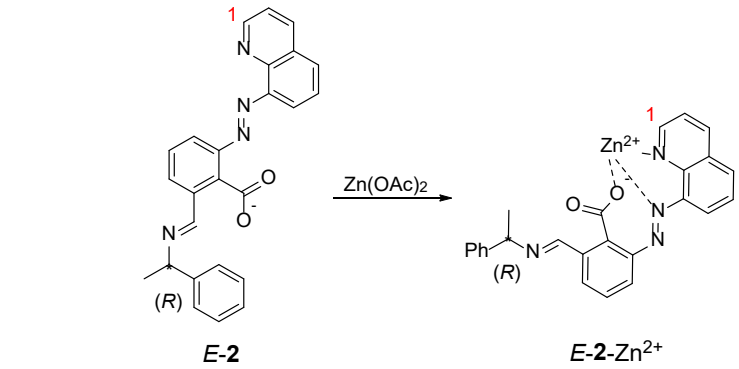

E-**2** *E*-**2**-Zn^{2+}

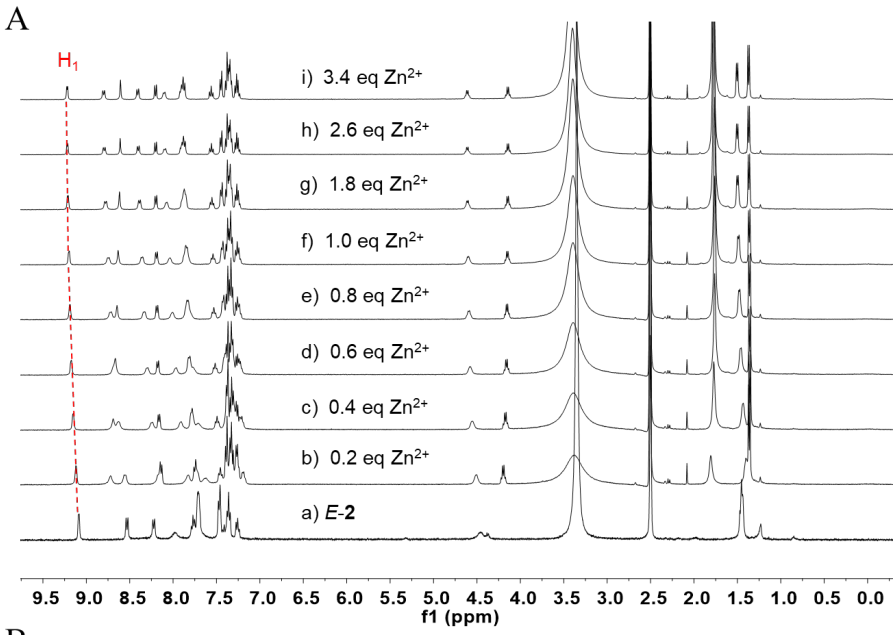

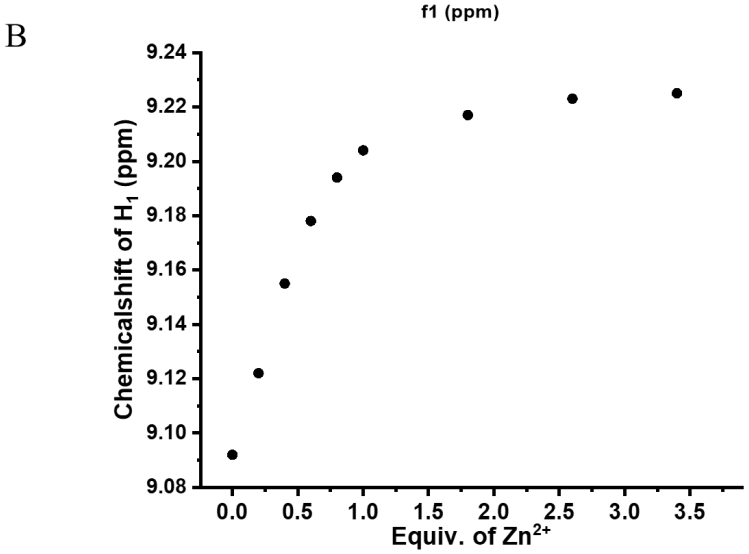

Figure S3. (A) Changes in ^{1}H NMR (400 MHz, 20 °C) spectrum upon titration of *E*-**2** (10 mM) with $Zn(OAc)_2 \cdot 2H_2O$ in DMSO-d_6. (B) The titration curve of panel A.

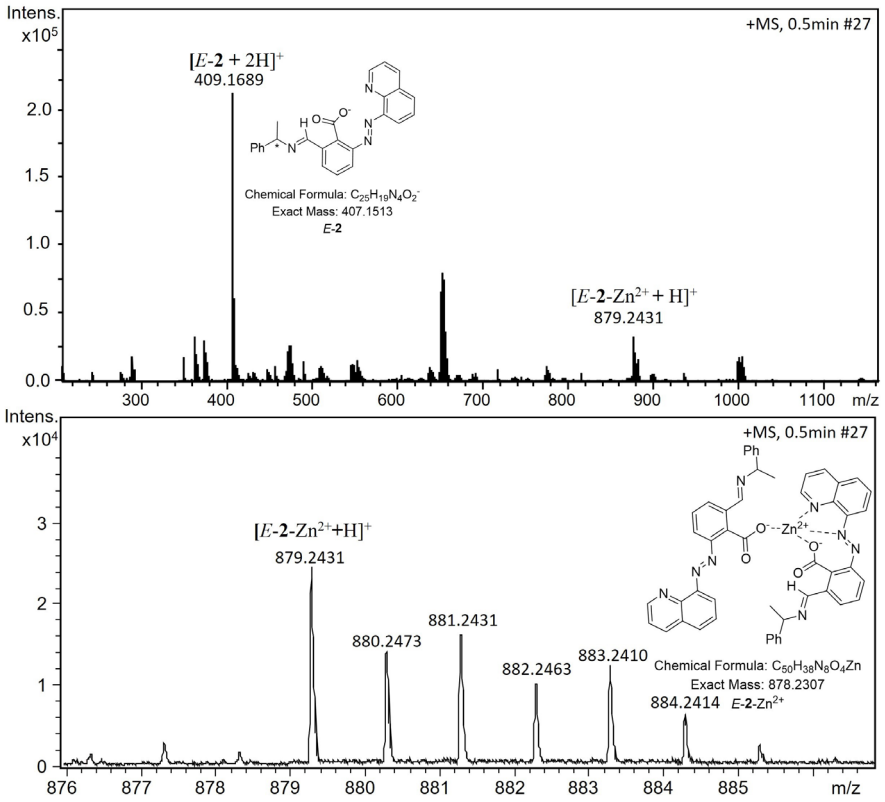

Figure S4. MS spectra of *E*-**2**-Zn^{2+}.

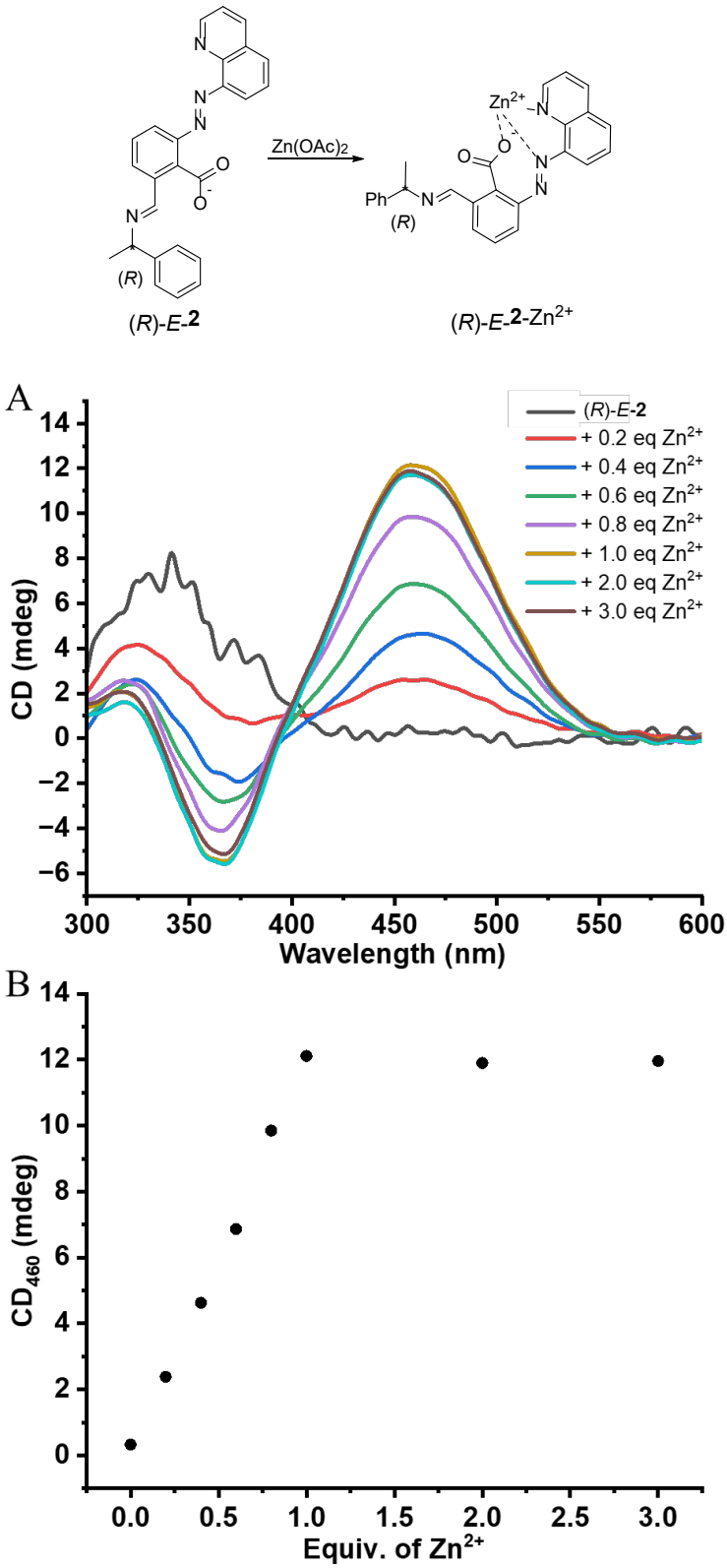

Figure S5. (A) CD spectra of (*R*)-*E*-**2** (0.10 mM) and after addition of $Zn(OAc)_2 \cdot 2H_2O$ in $CHCl_3$. (B) The titration isotherm (*R*)-*E*-**2** and $Zn(OAc)_2 \cdot 2H_2O$ in $CHCl_3$, as monitored by CD.

3. Effects of metal ions

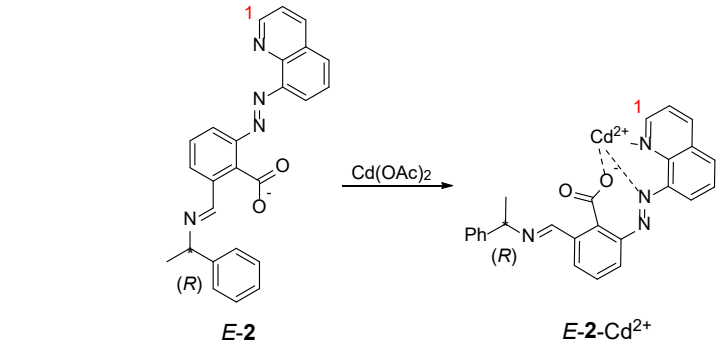

E-**2** *E*-**2**-Cd^{2+}

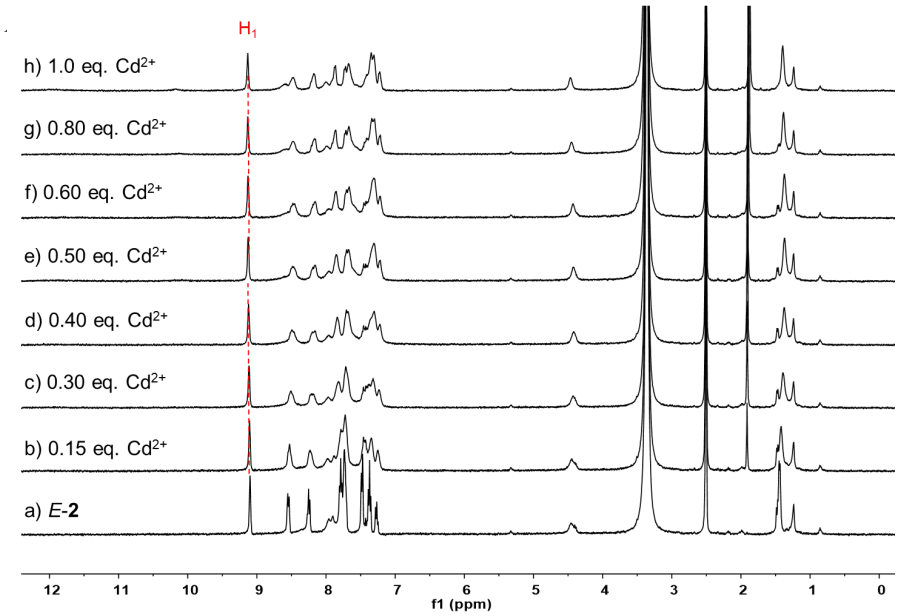

B

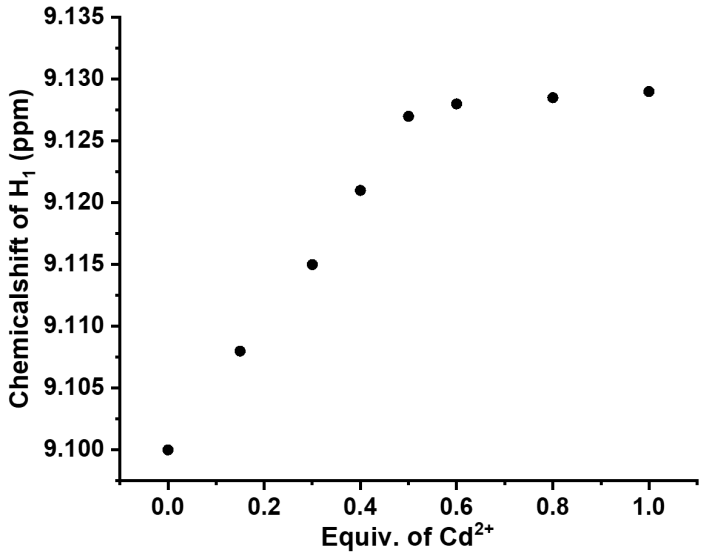

Figure S6. (A) Changes in ^{1}H NMR (400 MHz, 20 °C) spectrum upon titration of *E*-**2** (10 mM) with $Cd(OAc)_2 \cdot 2H_2O$ in DMSO-d_6. (B) The titration curve of panel A.

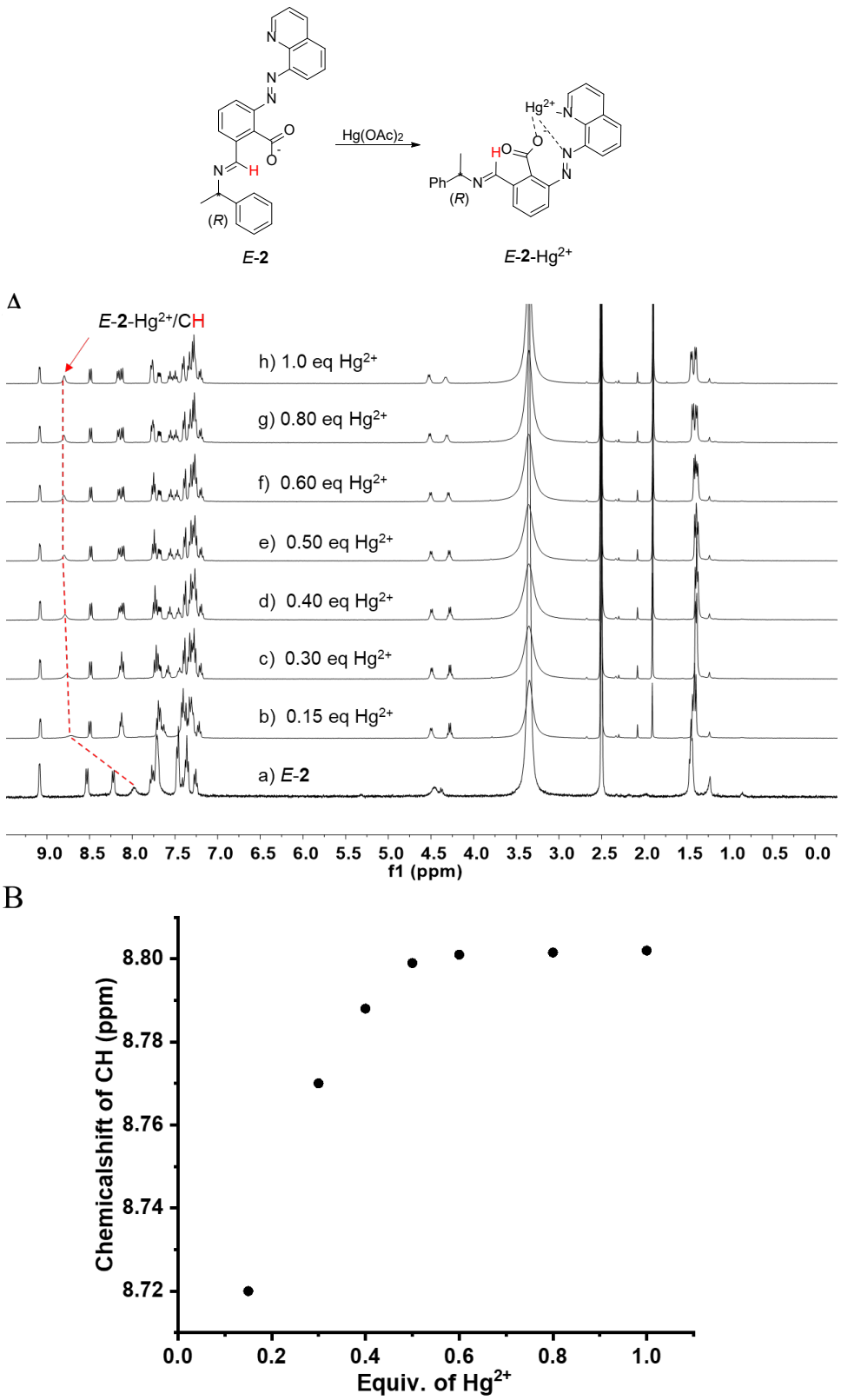

Figure S7. (A) Changes in ^{1}H NMR (400 MHz, 20 °C) spectrum upon titration of *E*-**2** (10 mM) with $Hg(OAc)_2 \cdot 2H_2O$ in DMSO-d_6. (B) The titration curve of panel A.

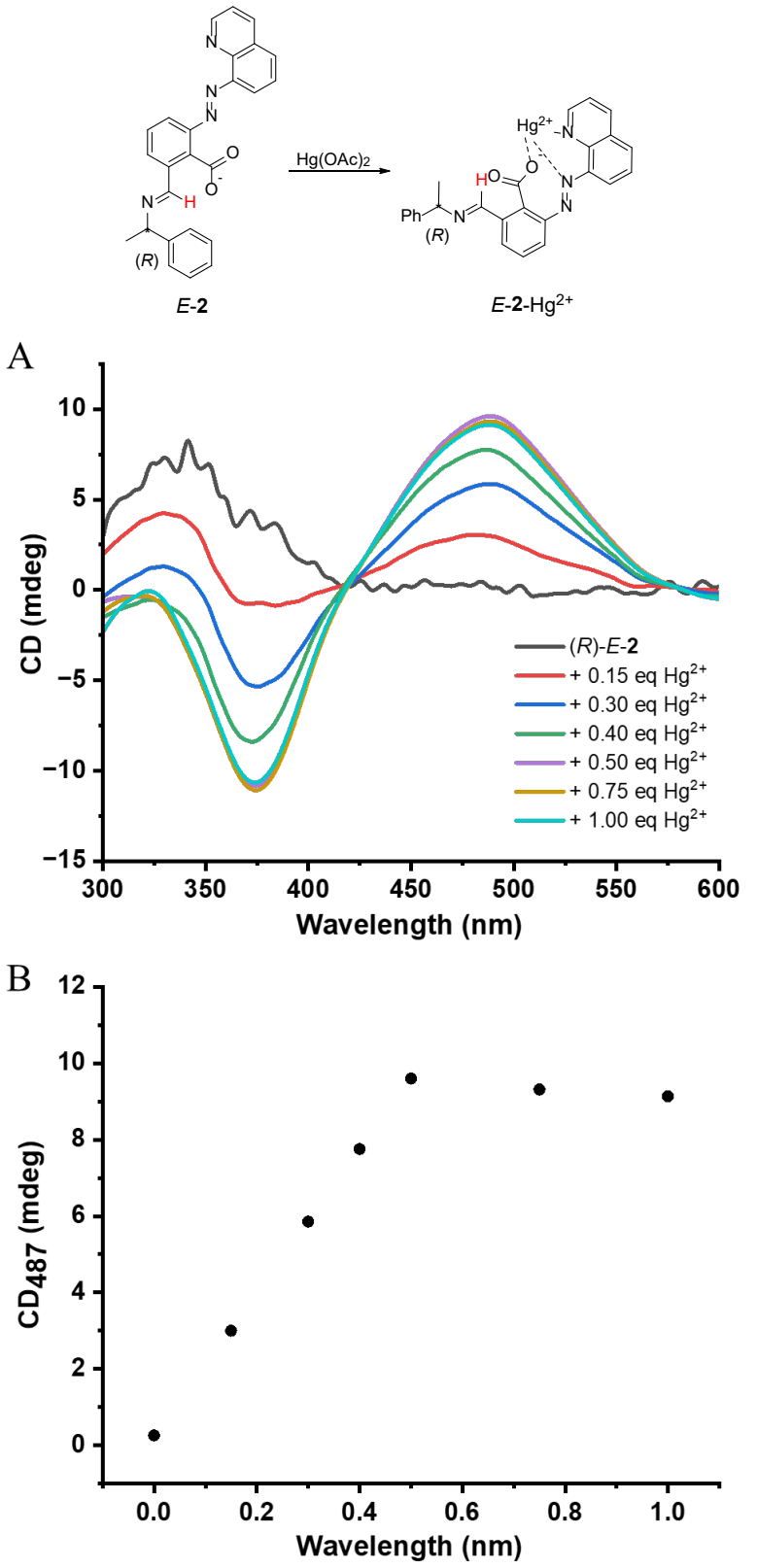

Figure S8. (A) CD spectra of (*R*)-*E*-**2** (0.10 mM) and after addition of $Hg(OAc)_2 \cdot 2H_2O$ in $CHCl_3$. (B) The titration isotherm (*R*)-*E*-**2** and $Hg(OAc)_2 \cdot 2H_2O$ in $CHCl_3$, as monitored by CD.

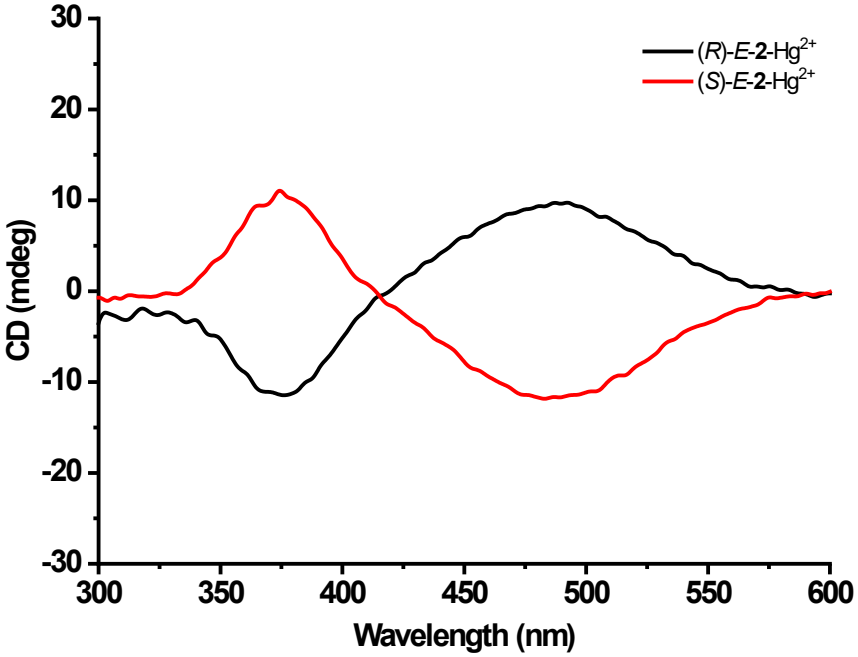

Figure S9. CD spectrum of *E*-**2**-Hg^{2+} (0.10 mM) in $CHCl_3$.

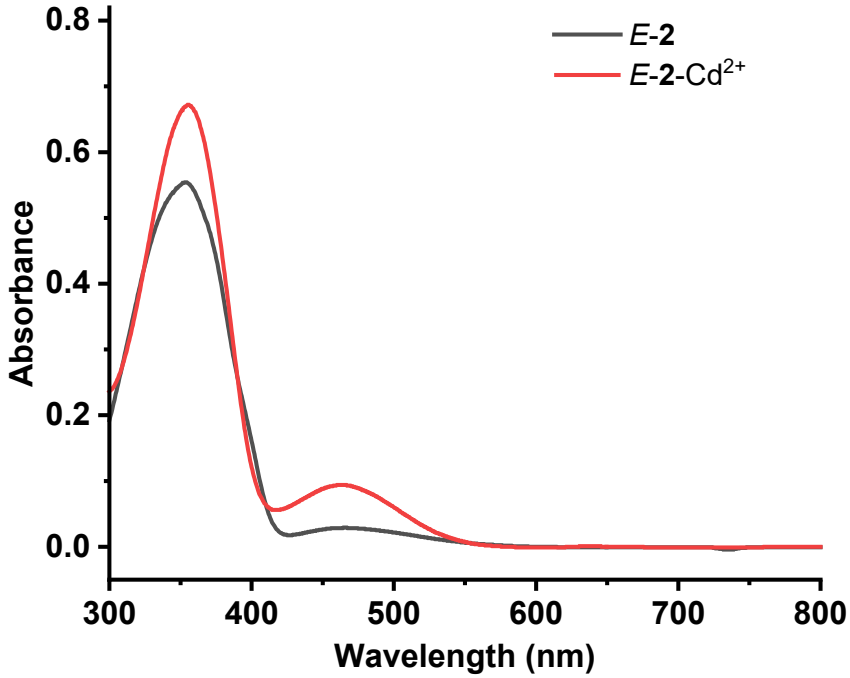

Figure S10. The UV spectra for *E*-**2** and *E*-**2**-Cd^{2+} in $CHCl_3$ (50 μM each).

Table S1. Calculated vertical excitation of major isomer in *E*-**2** and *E*-**2**-Cd^{2+} with oscillator strength (*f*) > 0.05 shown.

	Excited state	Transition character	*E* (nm)	MOs and Population (>10%)	*f*
E-**2**	S_1	n→π*	495	**HOMO-2 -> LUMO 43.17%** HOMO-1 -> LUMO 19.67% HOMO -> LUMO 21.42%	0.0781
	S_5	π→π*	323	**HOMO-4 -> LUMO 70.4%** HOMO -> LUMO+1 11.6%	0.4833
E-**2**-Cd^{2+}	S_2	n→π*	478	HOMO-4 -> LUMO 19.3% **HOMO -> LUMO 48.2%**	0.1257
	S_{10}	π→π*	358	**HOMO-4 -> LUMO 52.4%** HOMO -> LUMO+1 18.8%	0.4691

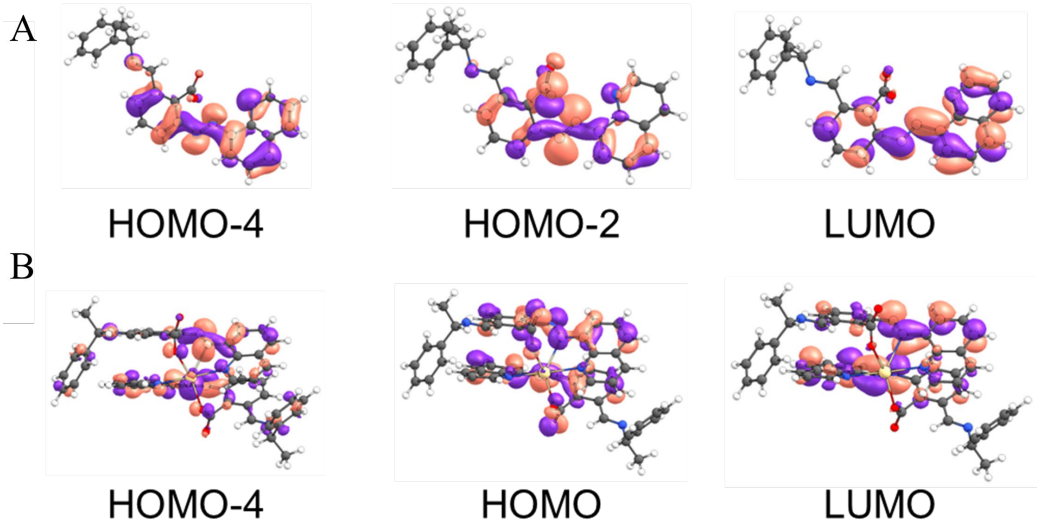

Figure S11. The major molecular orbitals involved with vertical excitation of *E*-**2** (A) and *E*-**2**-Cd^{2+} (B), respectively.

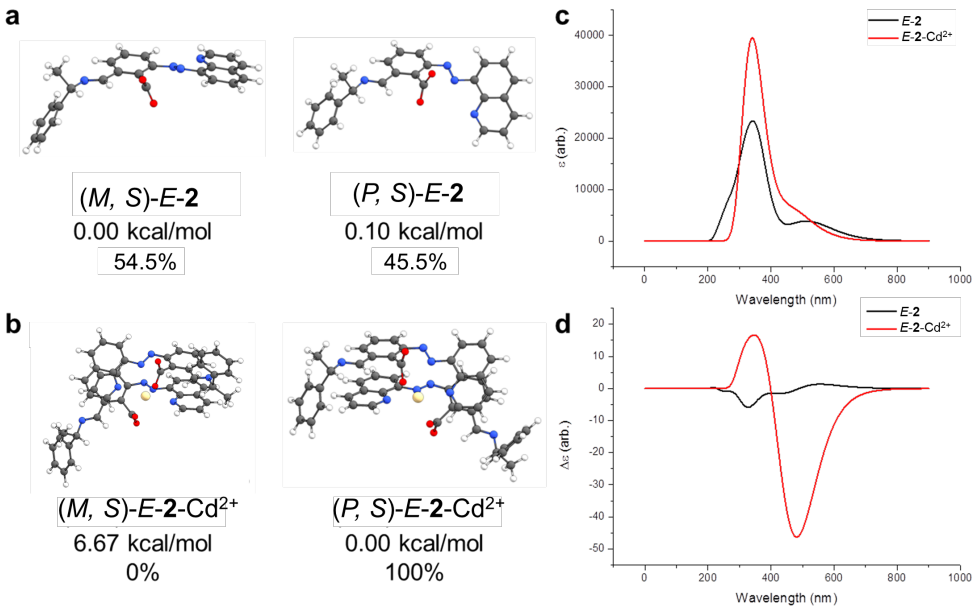

Figure S12. The calculated conformers of *E*-**2** and *E*-**2**-Cd^{2+} with the relative Gibbs energy and the conformational distribution shown (a and b). The calculated UV-vis (c) and CD (d) spectra for *E*-**2** and *E*-**2**-Cd^{2+}. For UV-vis and CD calculations, the averaged spectra were obtained by weighting the two conformers according to their conformational distribution. The calculated spectra echoed the experimental spectra. In calculated UV-vis spectra, two peaks were found for n→π* and π→π* excitation, which were confirmed by Table S1 and Figure S11.

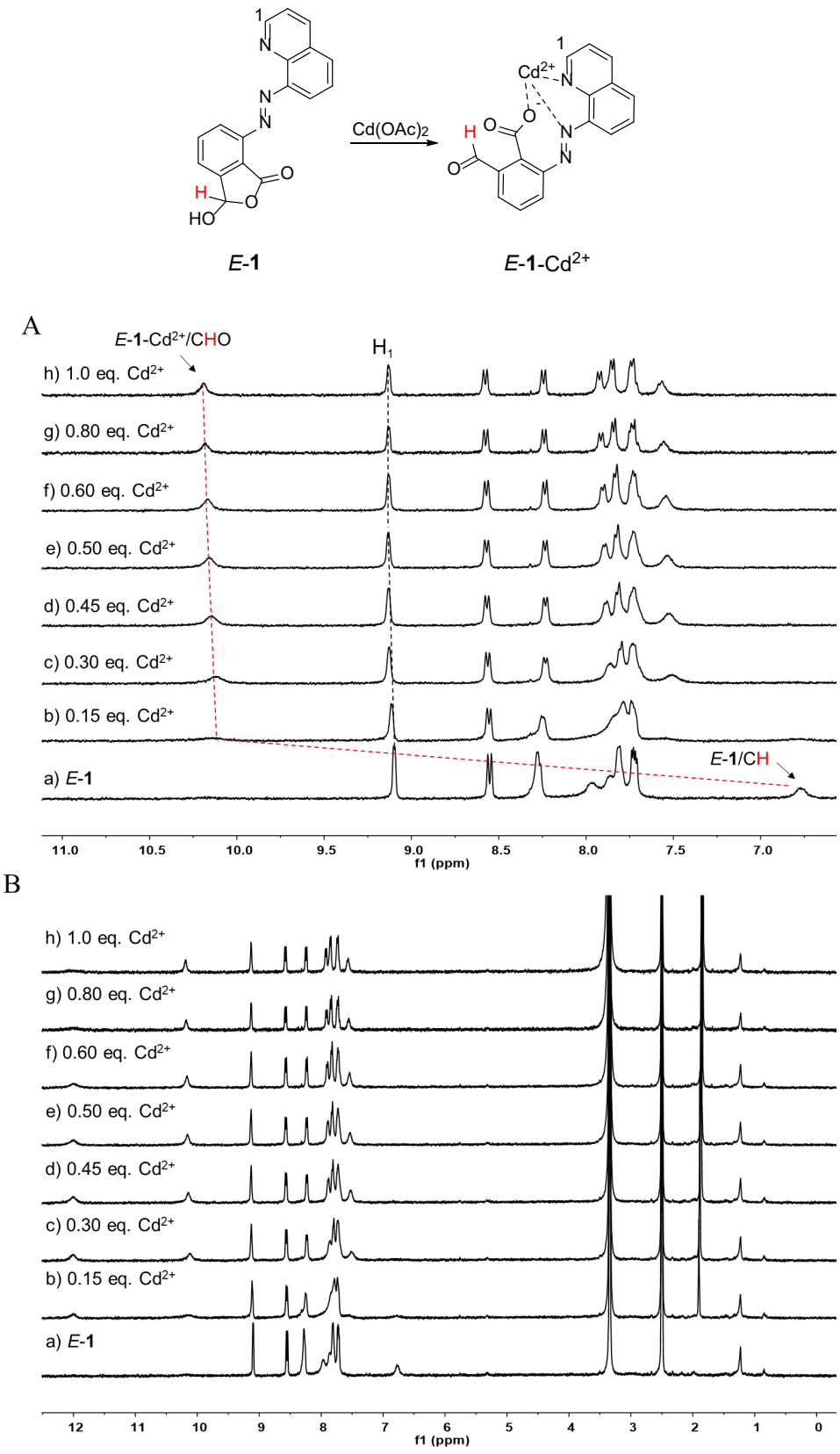

Figure S13. (A) Changes in ^{1}H NMR (400 MHz, 20 °C) spectrum upon titration of *E*-**1** (10 mM) with $Cd(OAc)_2 \cdot 2H_2O$ in DMSO-d_6. (B) The full ^{1}H NMR (400 MHz, 20 °C) spectrum of panel A.

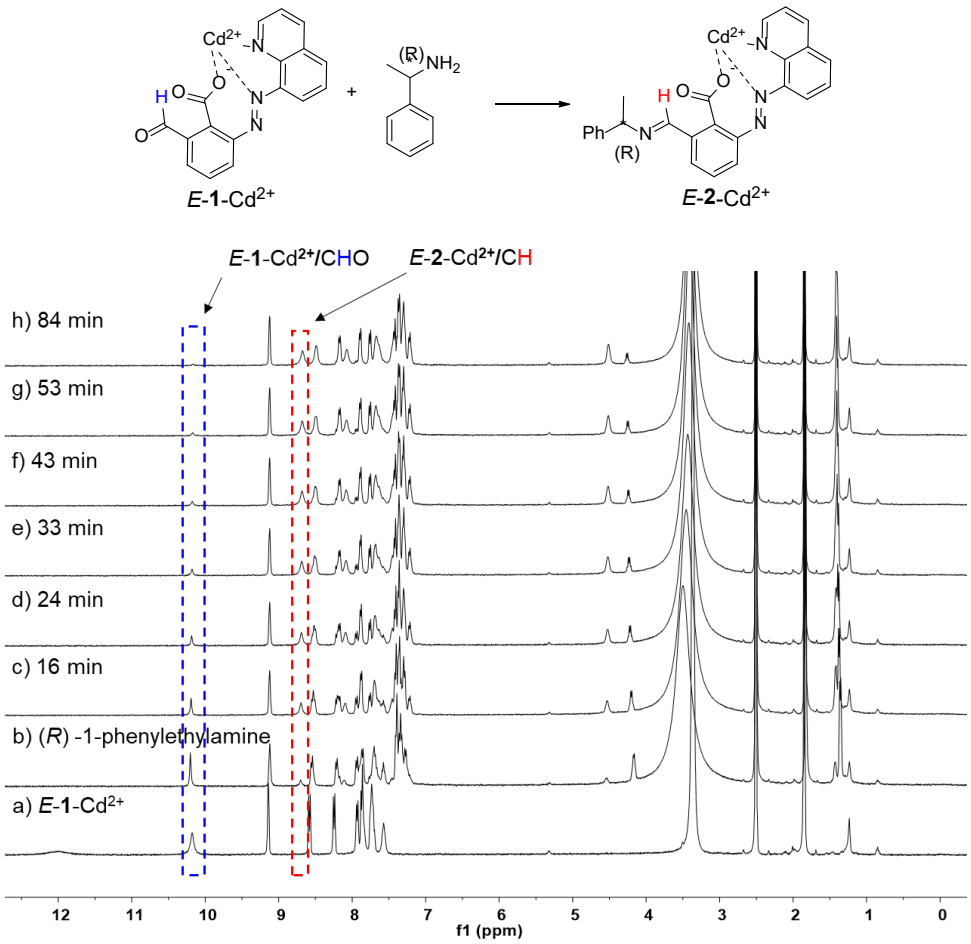

Figure S14. Changes in ^{1}H NMR (400 MHz, 20 ℃) spectrum of *E*-**1**-Cd^{2+} (10 mM) upon the reaction with (*R*)-1-phenylethylamine (1.5 equiv.) in DMSO-d_6.

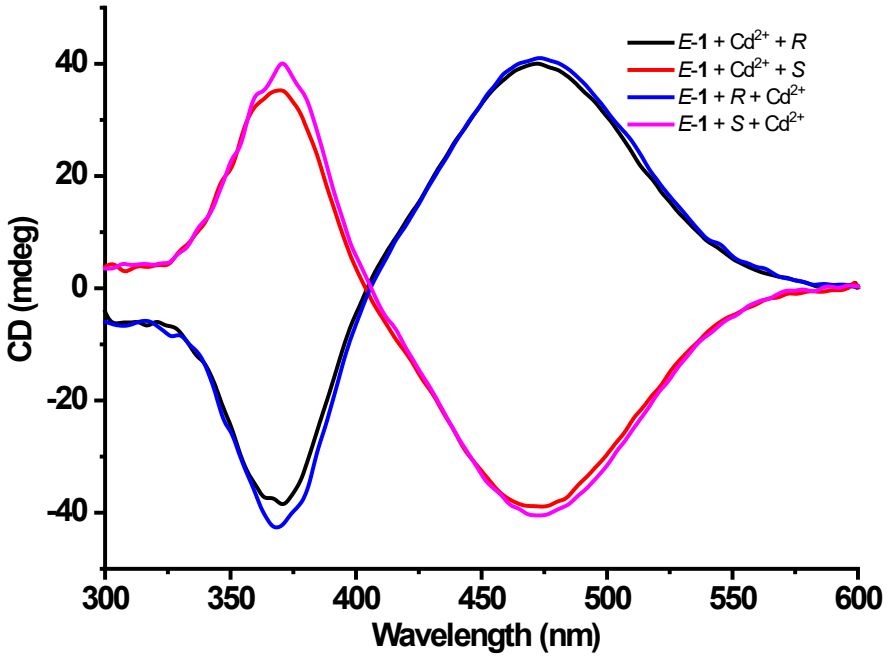

Figure S15. CD spectrum of *E*-**2**-Cd^{2+} (0.10 mM) obtained by different reaction pathways in $CHCl_3$.

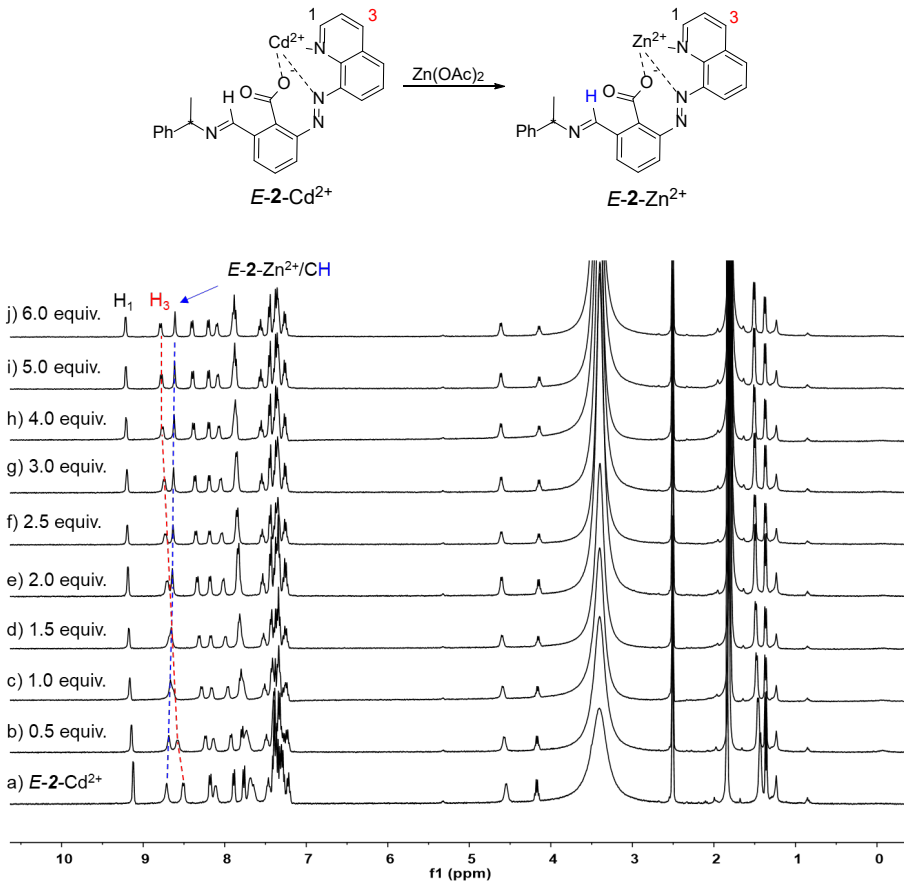

Figure S16. Changes in ^{1}H NMR (400 MHz, 20 °C) spectrum upon titration of *E*-**2**-Cd^{2+} (10 mM) with $Zn(OAc)_2{\cdot}2H_2O$ in DMSO-d_6.

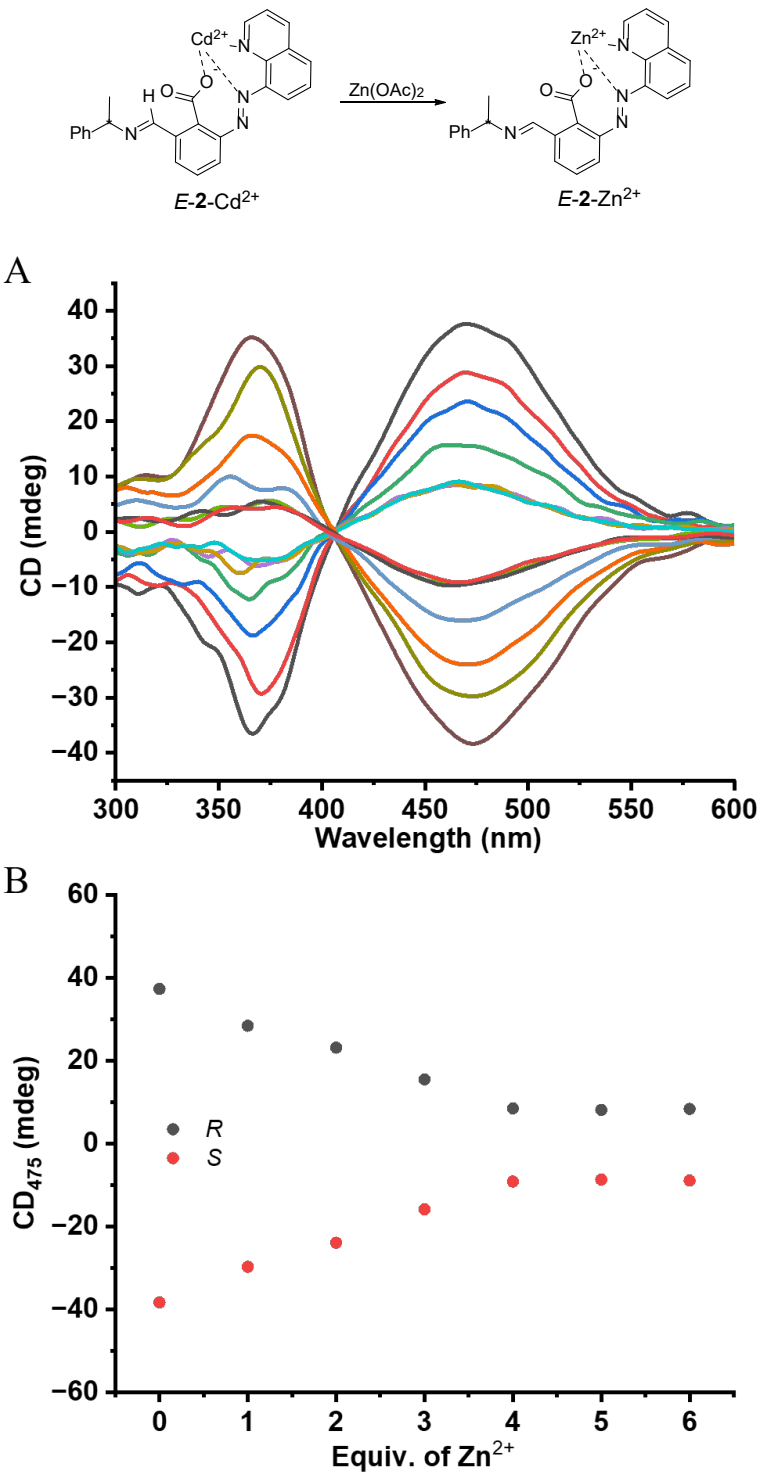

Figure S17. (A) CD spectra of (*R*)/(*S*)-*E*-**2**-Cd^{2+} (0.10 mM) and after addition of $Zn(OAc)_2 \cdot 2H_2O$ in $CHCl_3$. (B) The titration isotherm (*R*)/(*S*)-*E*-**2**-Cd^{2+} and $Zn(OAc)_2 \cdot 2H_2O$ in $CHCl_3$, as monitored by CD.

4. Effects of photo-modulation

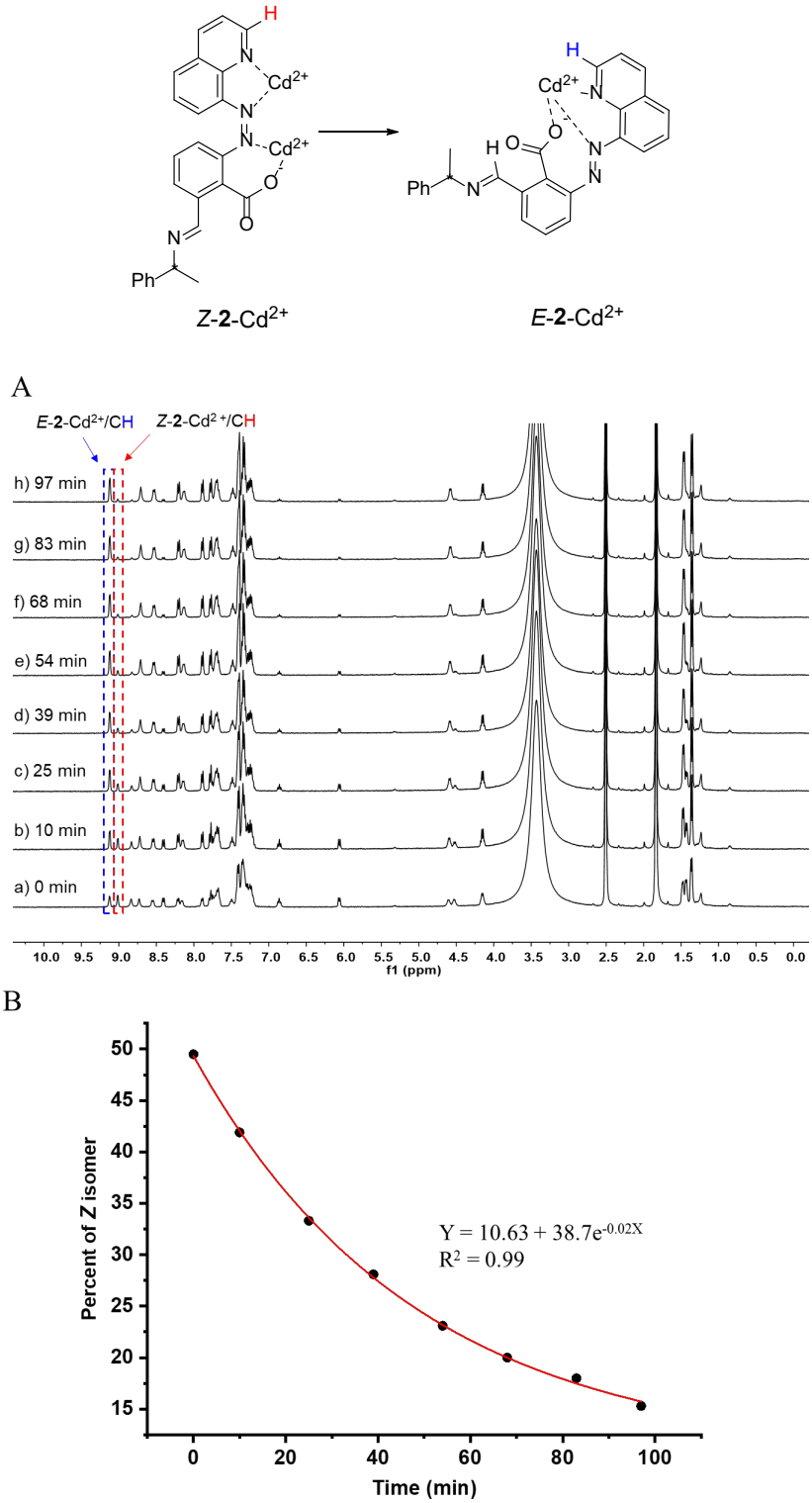

Figure S18. Changes in ^{1}H NMR (400 MHz, 20 °C) spectrum (A) as well as thermal isomerization kinetic curve (B) after the irradiation of *E*-**2**-Cd^{2+} (10 mM) in DMSO-d_6 for 1.5 h at 365 nm (the percent of *Z*-**2**-Cd^{2+} is 49% after irradiation for 1.5 h) and then waiting in the dark (25 ºC) at varied time. The half-life of *Z*-**2**-Cd^{2+} was determined to be 33 min at 25 ºC.

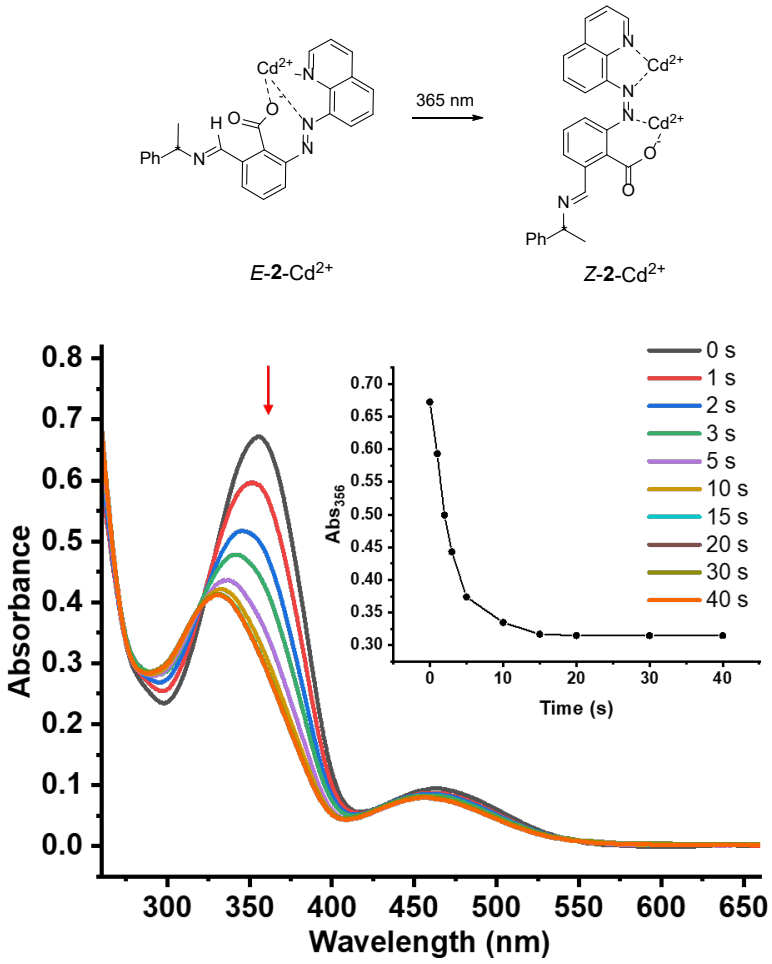

Figure S19. Photoisomerization of *E*-**2**-Cd^{2+} to give *Z*-**2**-Cd^{2+}: changes in absorption spectra upon irradiation of *E*-**2**-Cd^{2+} (50 μM in $CHCl_3$) with 365 nm light. Inset: the photoisomerization kinetic curve of *E*-**2**-Cd^{2+}, via monitoring the absorbance at 356 nm.

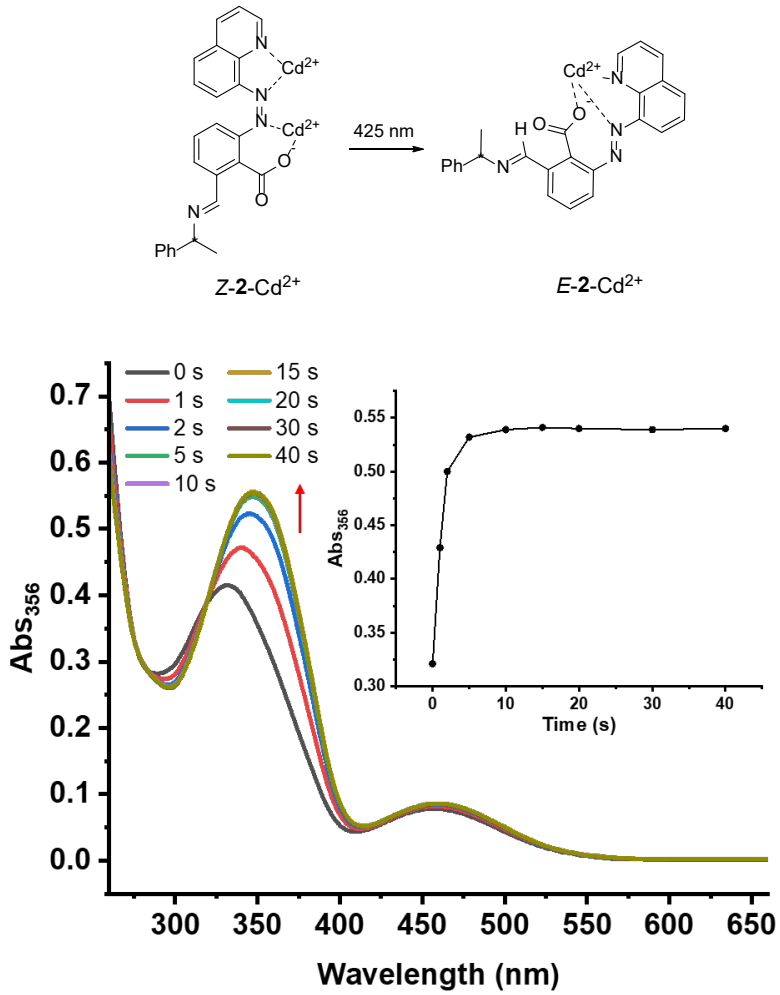

Figure S20. Photoisomerization of *Z*-**2**-Cd^{2+} (created through irradiation of *E*-**2**-Cd^{2+} at 365 nm) to give *E*-**2**-Cd^{2+}: changes in absorption spectra upon irradiation of *Z*-**2**-Cd^{2+} (50 μM in $CHCl_3$) with 425 nm light. Inset: the photoisomerization kinetic curve of *Z*-**2**-Cd^{2+}, via monitoring the absorbance at 356 nm.

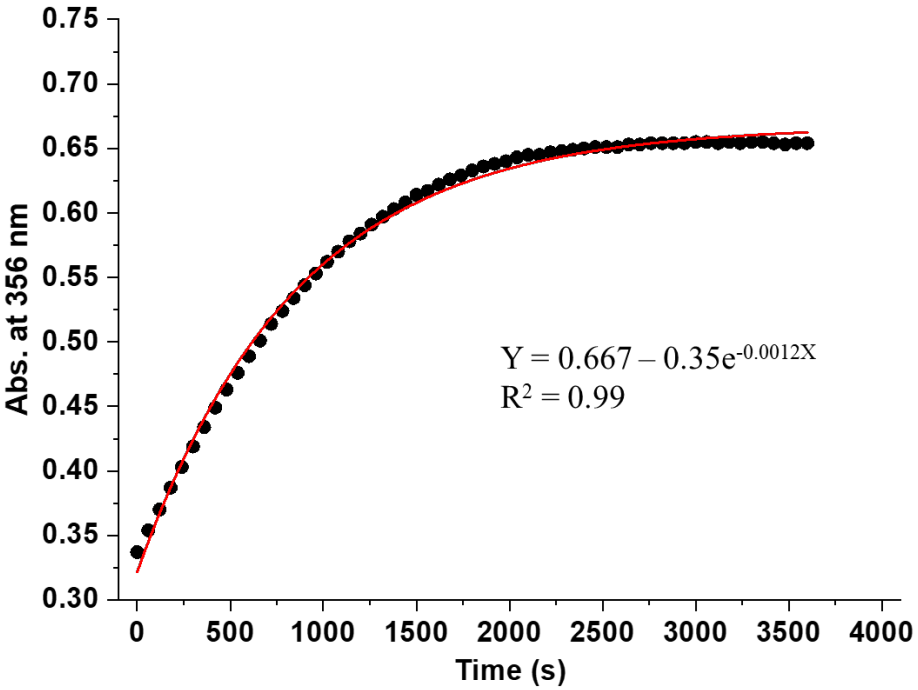

Figure S21. Changes in absorption at 356 nm after the irradiation of *E*-**2**-Cd^{2+} (50 μM) in $CHCl_3$ for 2 min at 365 nm and then waiting in the dark (25 ºC) at varied time. The half-life of *Z*-**2**-Cd^{2+} was determined to be 10 min at 25 ºC.

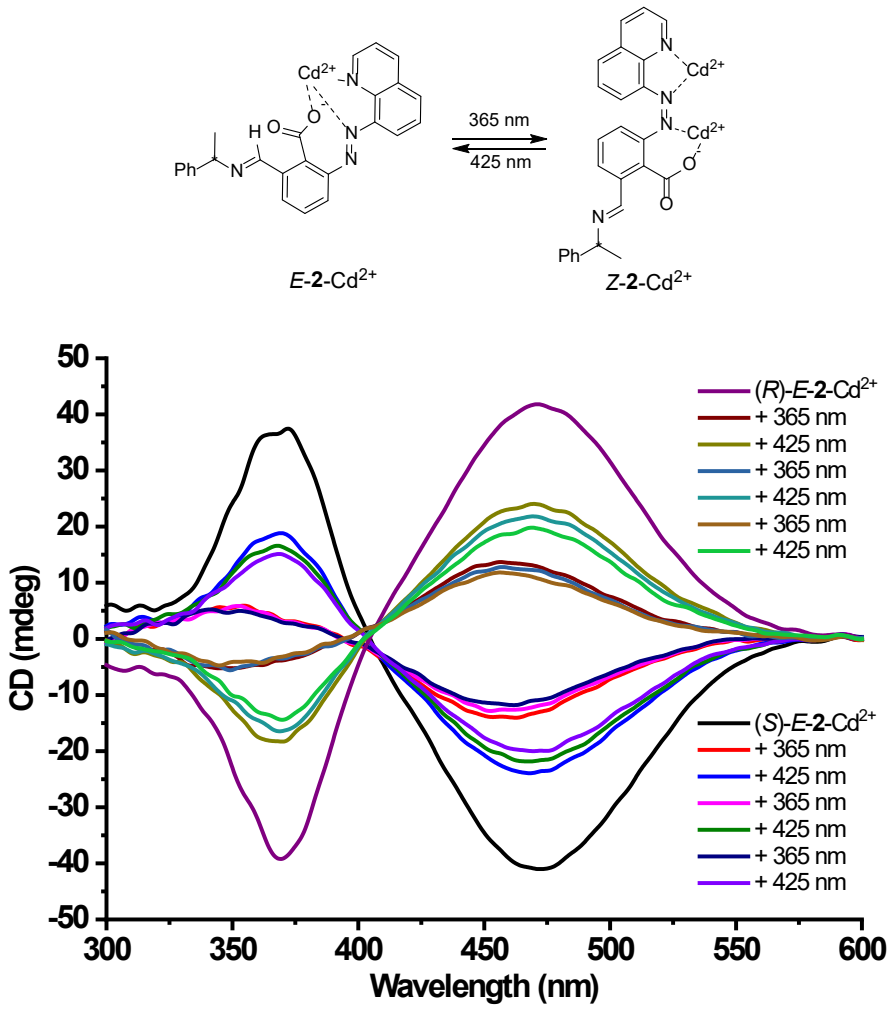

Figure S22. CD spectra of *E*-**2**-Cd^{2+} (0.10 mM) and after alternative irradiation at 365 and 425 nm in $CHCl_3$.

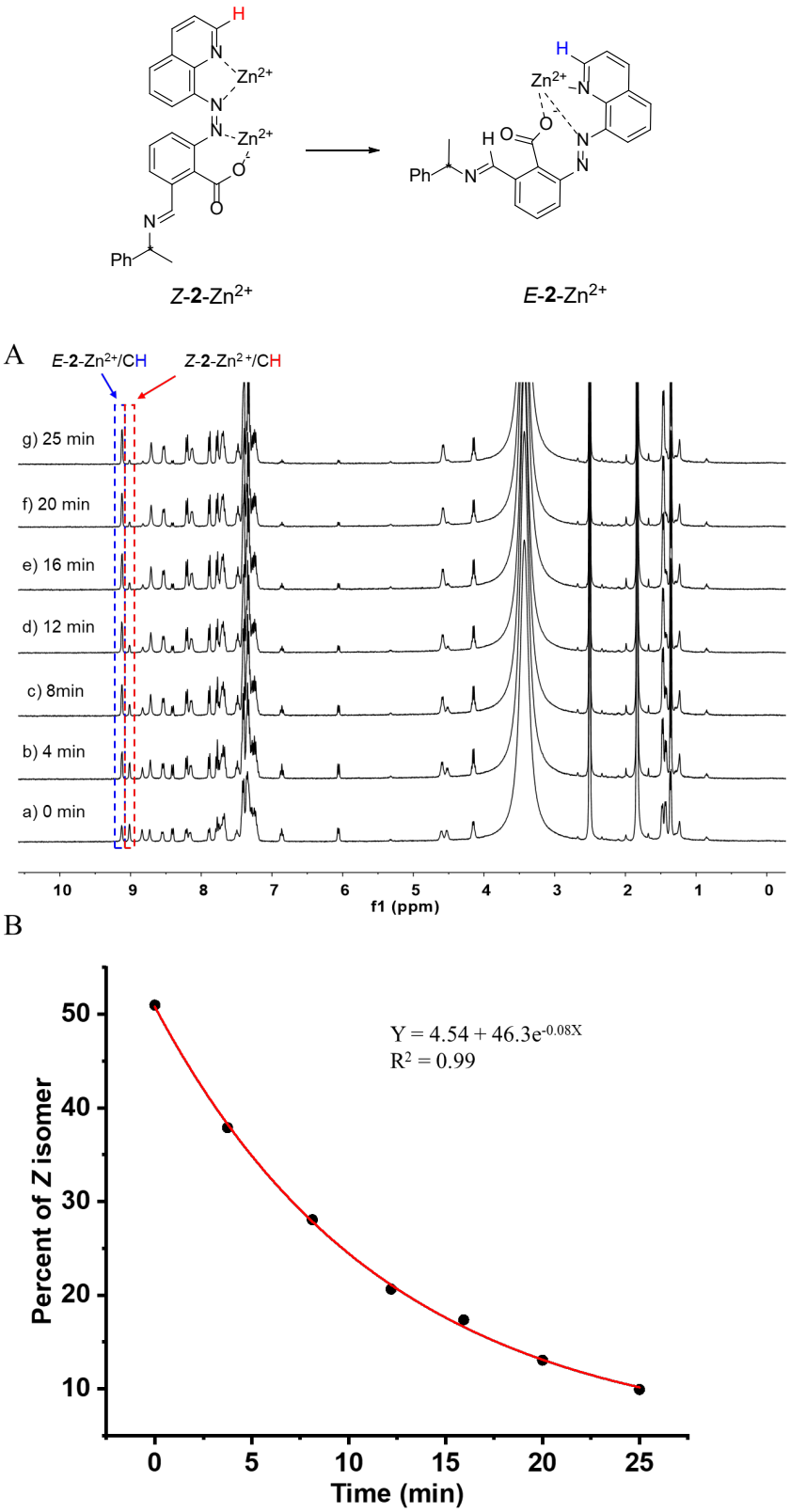

Figure S23. Changes in ^{1}H NMR (400 MHz, 20 ℃) spectrum (A) as well as thermal isomerization kinetic curve (B) after the irradiation of *E*-**2**-Zn^{2+} (10 mM) in DMSO-d_6 for 1.5 h at 365 nm (the percent of *Z*-**2**-Zn^{2+} is 51% after irradiation for 1.5 h) and then waiting in the dark (25 ºC) at varied time. The half-life of *Z*-**2**-Zn^{2+} was determined to be 9 min at 25 ºC.

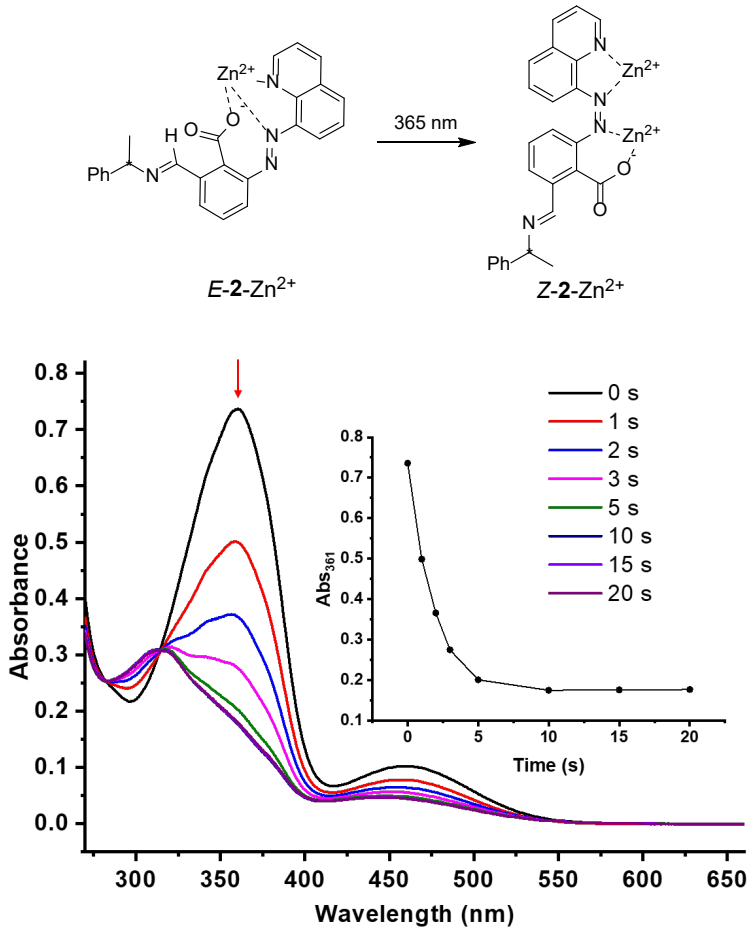

Figure S24. Photoisomerization of *E*-**2**-Zn^{2+} to give *Z*-**2**-Zn^{2+}: changes in absorption spectra upon irradiation of *E*-**2**-Zn^{2+} (50 μM in $CHCl_3$) with 365 nm light. Inset: the photoisomerization kinetic curve of *E*-**2**-Zn^{2+}, via monitoring the absorbance at 361 nm.

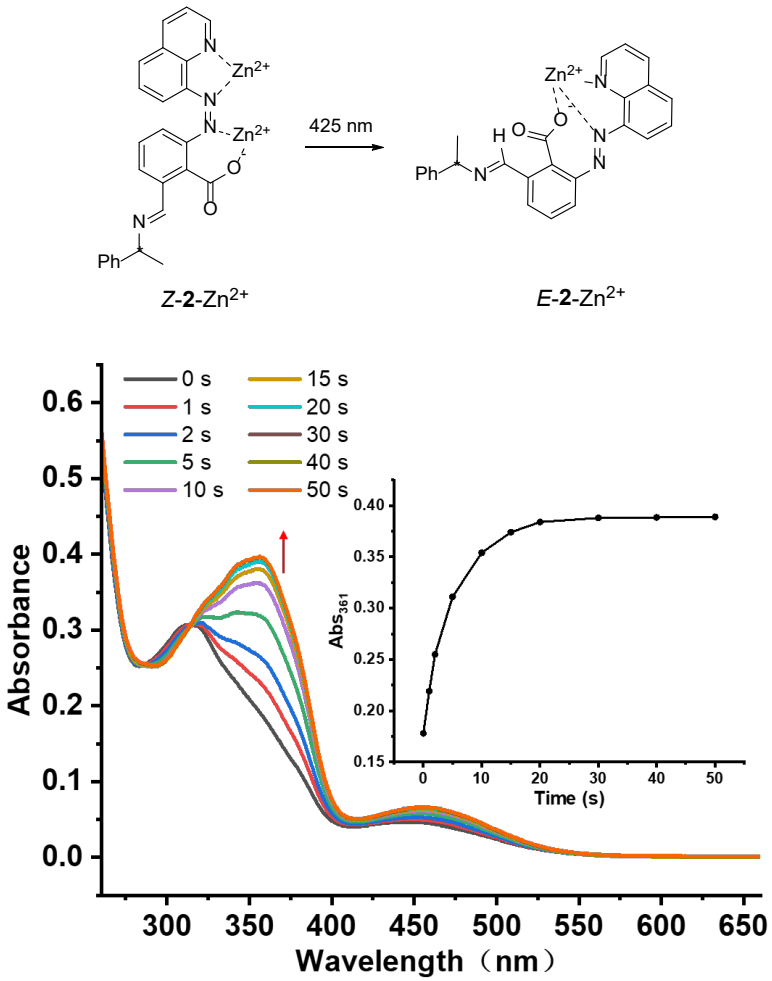

Figure S25. Photoisomerization of *Z*-**2**-Zn^{2+} (created through irradiation of *E*-**2**-Zn^{2+} at 365 nm) to give *E*-**2**-Zn^{2+}: changes in absorption spectra upon irradiation of *Z*-**2**-Zn^{2+} (50 μM in $CHCl_3$) with 425 nm light. Inset: the photoisomerization kinetic curve of *Z*-**2**-Zn^{2+}, via monitoring the absorbance at 361 nm.

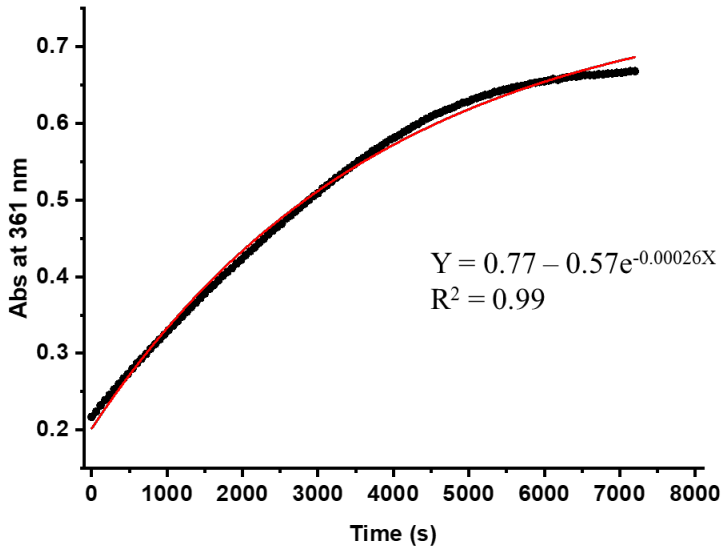

Figure S26. Changes in absorption at 361 nm after the irradiation of *E*-**2**-Zn^{2+} (10 mM) in $CHCl_3$ for 2 min at 365 nm and then waiting in the dark (25 ºC) at varied time. The half-life of *Z*-**2**-Zn^{2+} was determined to be 45 min at 25 ºC.

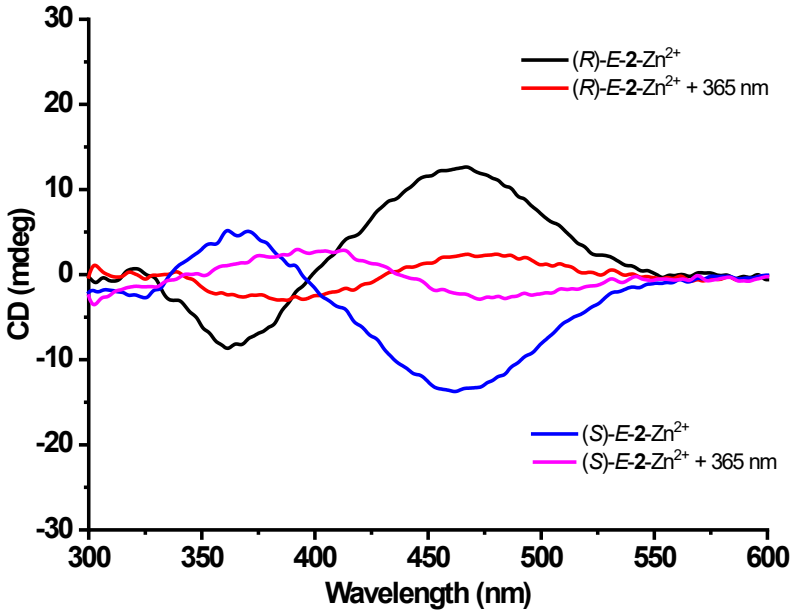

Figure S27. CD spectrum of *E*-**2**-Zn^{2+} (0.10 mM) and after irradiation for 2 min with 365 nm light in $CHCl_3$.

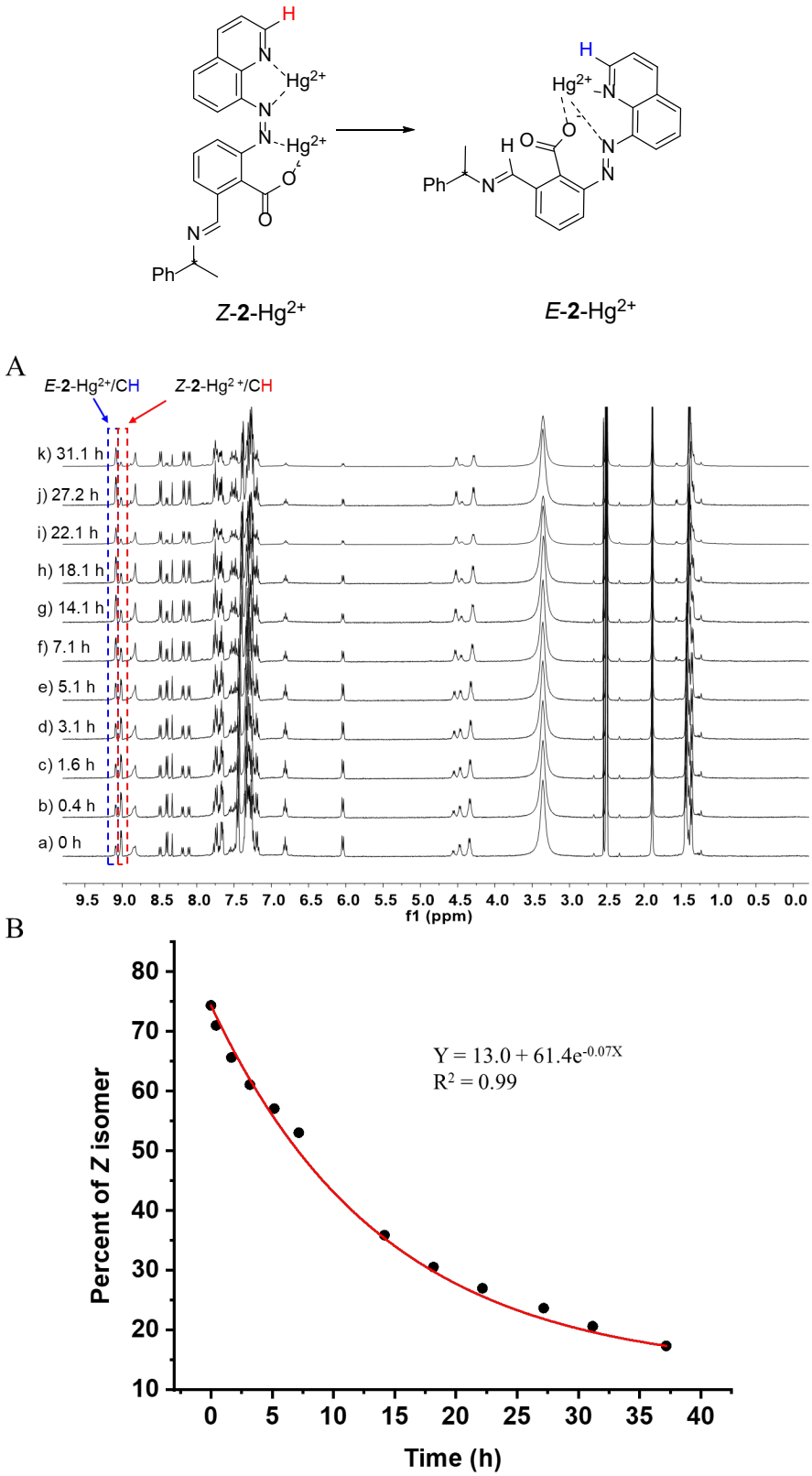

Figure S28. Changes in ^{1}H NMR (400 MHz, 20 ℃) spectrum (A) as well as thermal isomerization kinetic curve (B) after the irradiation of *E*-**2**-Hg^{2+} (10 mM) in DMSO-d_6 for 45 min at 365 nm (the percent of *Z*-**2**-Hg^{2+} is 73% after irradiation for 45 min) and then waiting in the dark (25 ºC) at varied time. The half-life of *Z*-**2**-Hg^{2+} was determined to be 9.4 h at 25 ºC.

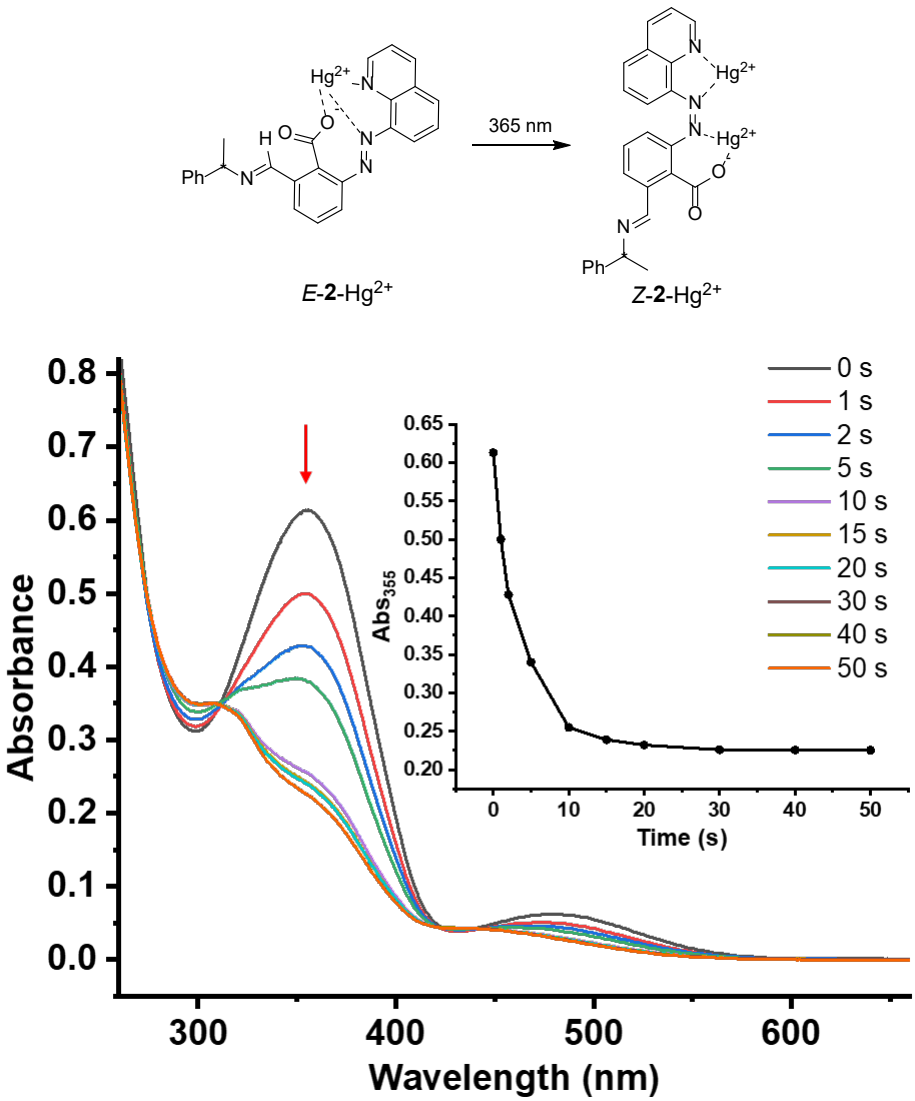

Figure S29. Photoisomerization of *E*-**2**-Hg^{2+} to give *Z*-**2**-Hg^{2+}: changes in absorption spectra upon irradiation of *E*-**2**-Hg^{2+} (50 μM in $CHCl_3$) with 365 nm light. Inset: the photoisomerization kinetic curve of *E*-**2**-Hg^{2+}, via monitoring the absorbance at 355 nm.

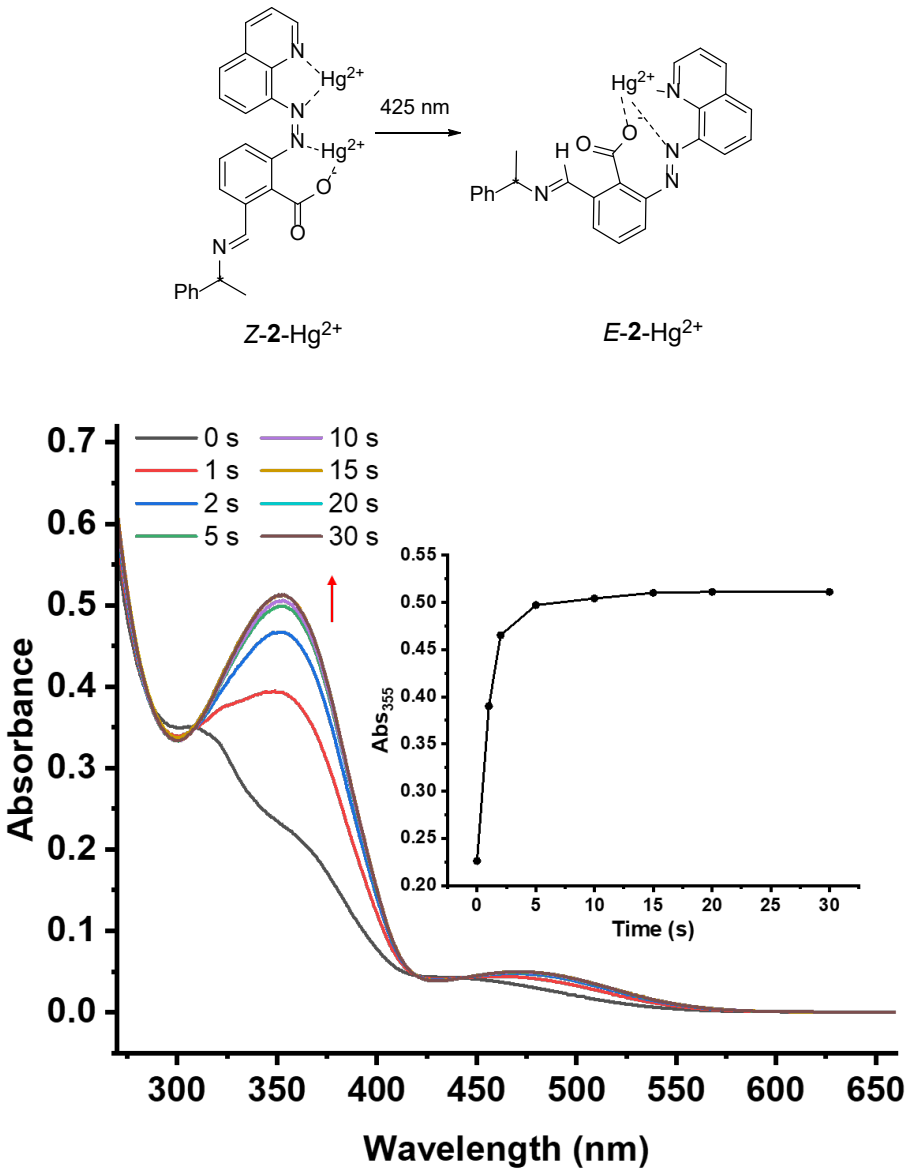

Figure S30. Photoisomerization of *Z*-**2**-Hg^{2+} (created through irradiation of *E*-**2**-Hg^{2+} at 365 nm) to give *E*-**2**-Hg^{2+}: changes in absorption spectra upon irradiation of *Z*-**2**-Hg^{2+} (50 μM in $CHCl_3$) with 425 nm light. Inset: the photoisomerization kinetic curve of *Z*-**2**-Hg^{2+}, via monitoring the absorbance at 355 nm.

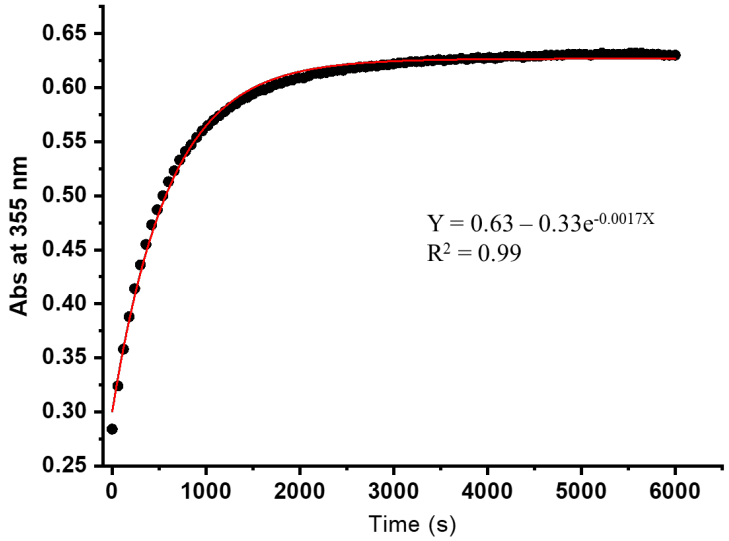

Figure S31. Changes in absorption at 355 nm after the irradiation of *E*-**2**-Hg^{2+} (10 mM) in $CHCl_3$ for 2 min at 365 nm and then waiting in the dark (25 ºC) at varied time. The half-life of *Z*-**2**-Hg^{2+} was determined to be 7 min at 25 ºC.

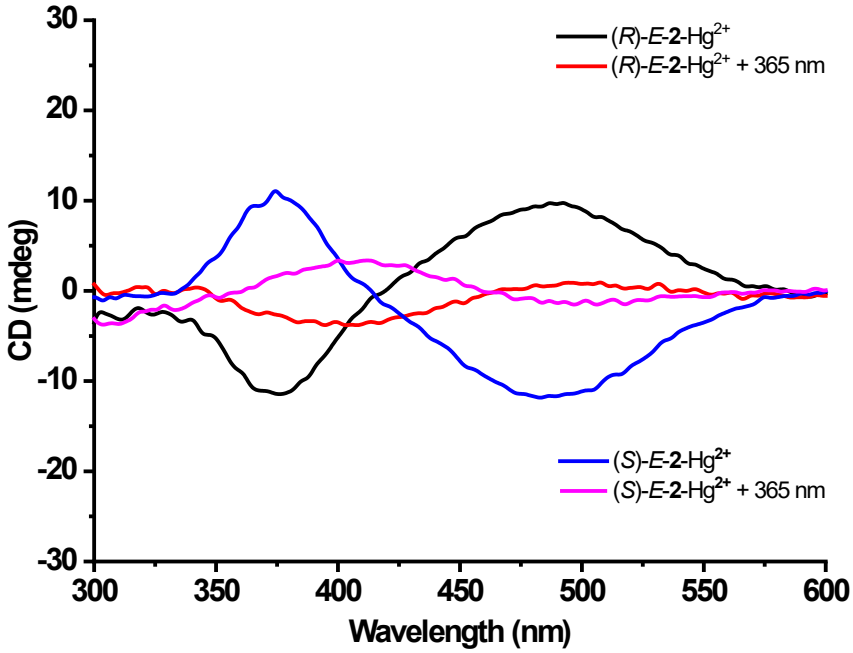

Figure S32. CD spectrum of *E*-**2**-Hg^{2+} (0.10 mM) and after irradiation for 2 min with 365 nm light in $CHCl_3$.

(*M, S*)-*Z*-**2**-Cd^{2+}
0.00 kcal/mol
68.2%

(*P, S*)-*Z*-**2**-Cd^{2+}
0.45 kcal/mol
31.8%

Figure S33. The calculated structures of (*M*, *S*)-*Z*-**2**-Cd^{2+} and (*M*, *R*)-*Z*-**2**-Cd^{2+}, with the relative Gibbs energy and the conformational distribution shown.

5. The regulation with dynamic covalent chemistry

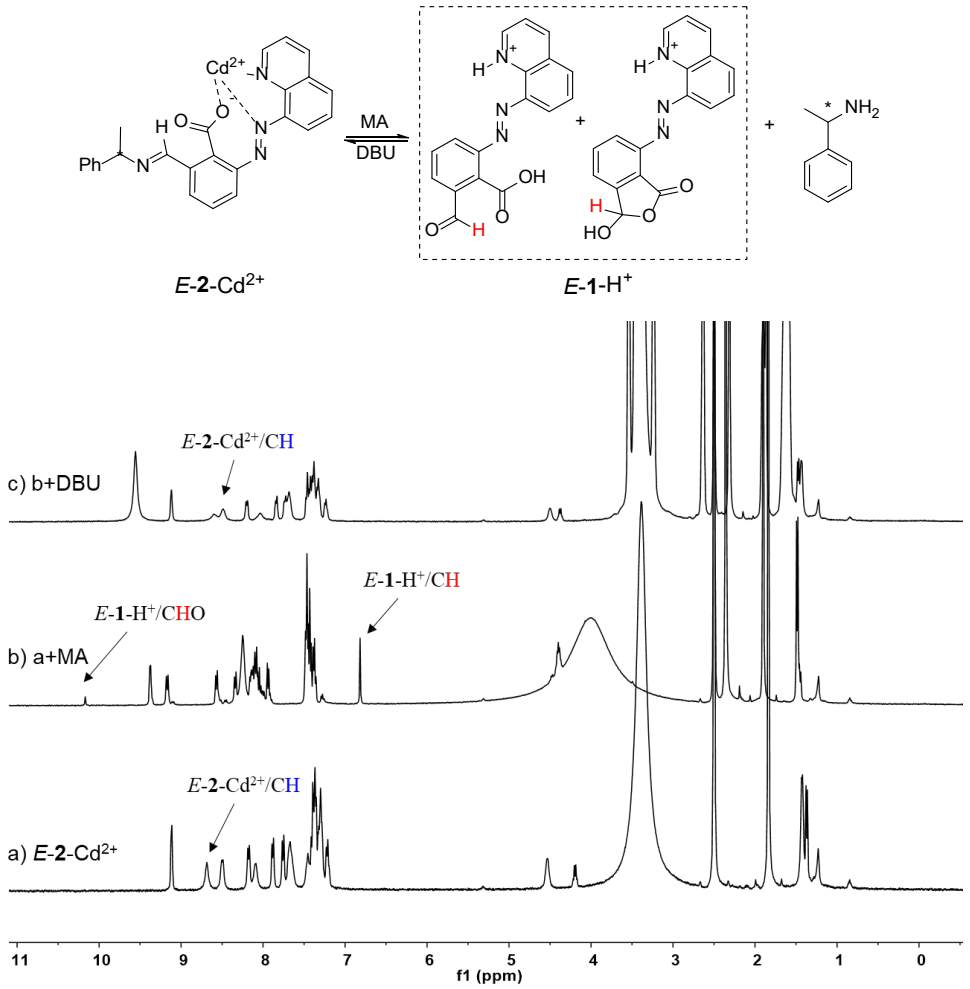

Figure S34. ^{1}H NMR (400 MHz, 20 °C) spectra of *E*-**2**-Cd^{2+} (10 mM) (a) and after addition of 5.0 equiv. MA (b) and then 5.0 equiv. DBU (c) in DMSO-d_6.

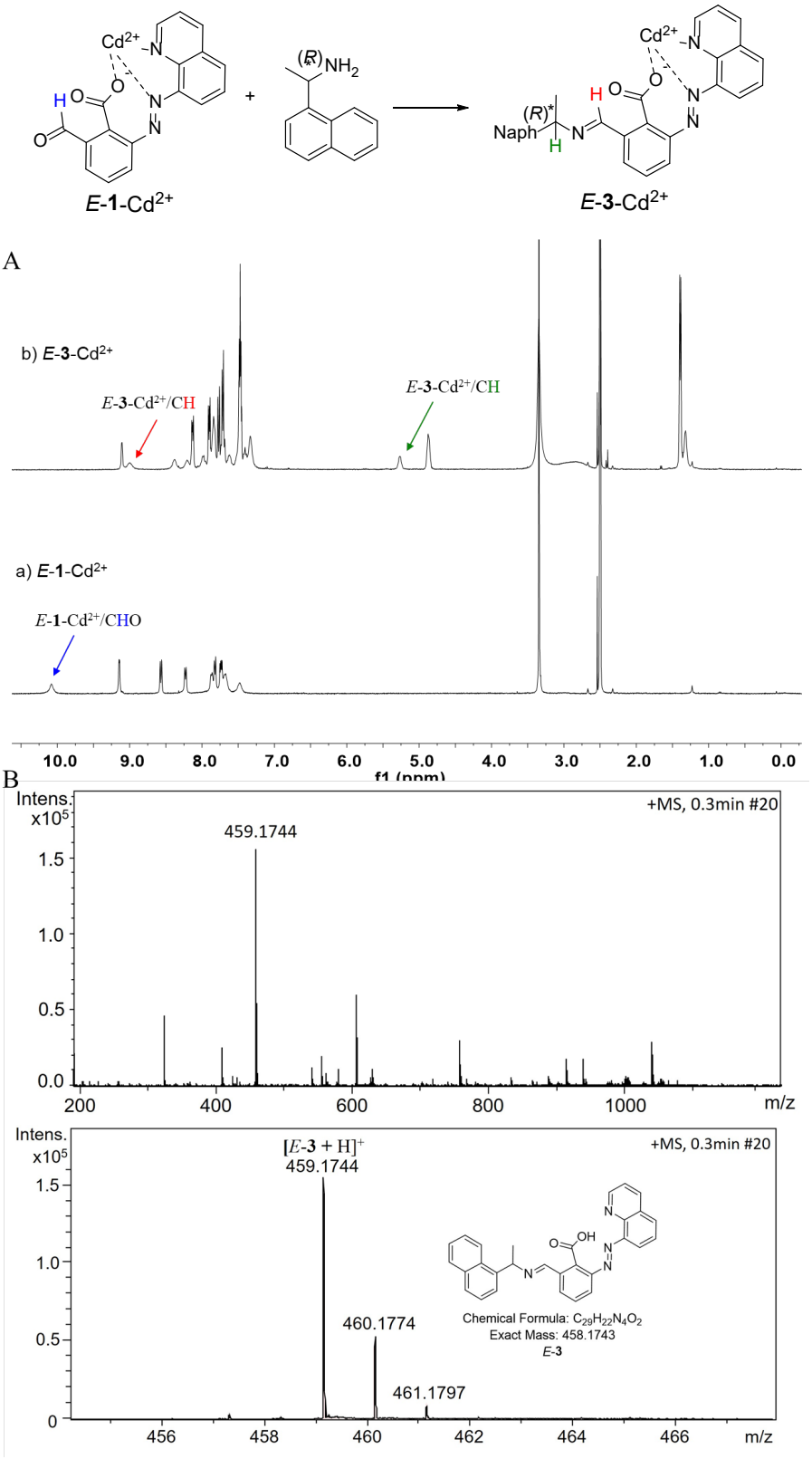

Figure S35. (A) ^{1}H NMR (400 MHz, 20 °C) spectrum of *E*-**1**-Cd^{2+} (10 mM) (a) and after addition of 1.5 equiv. of (*R*)-1-(1-naphthyl)ethylamine (b) in DMSO-d_6. The reaction reached equilibrium within 1.5 h. (B) MS spectra of *E*-**3**.

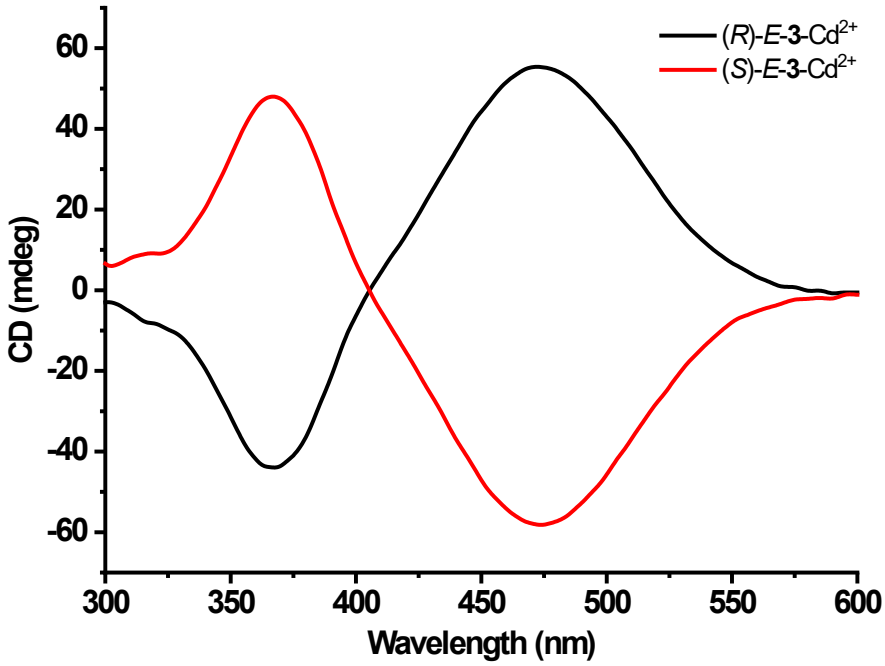

Figure S36. CD spectrum of *E*-**3**-Cd^{2+} (0.10 mM) in $CHCl_3$.

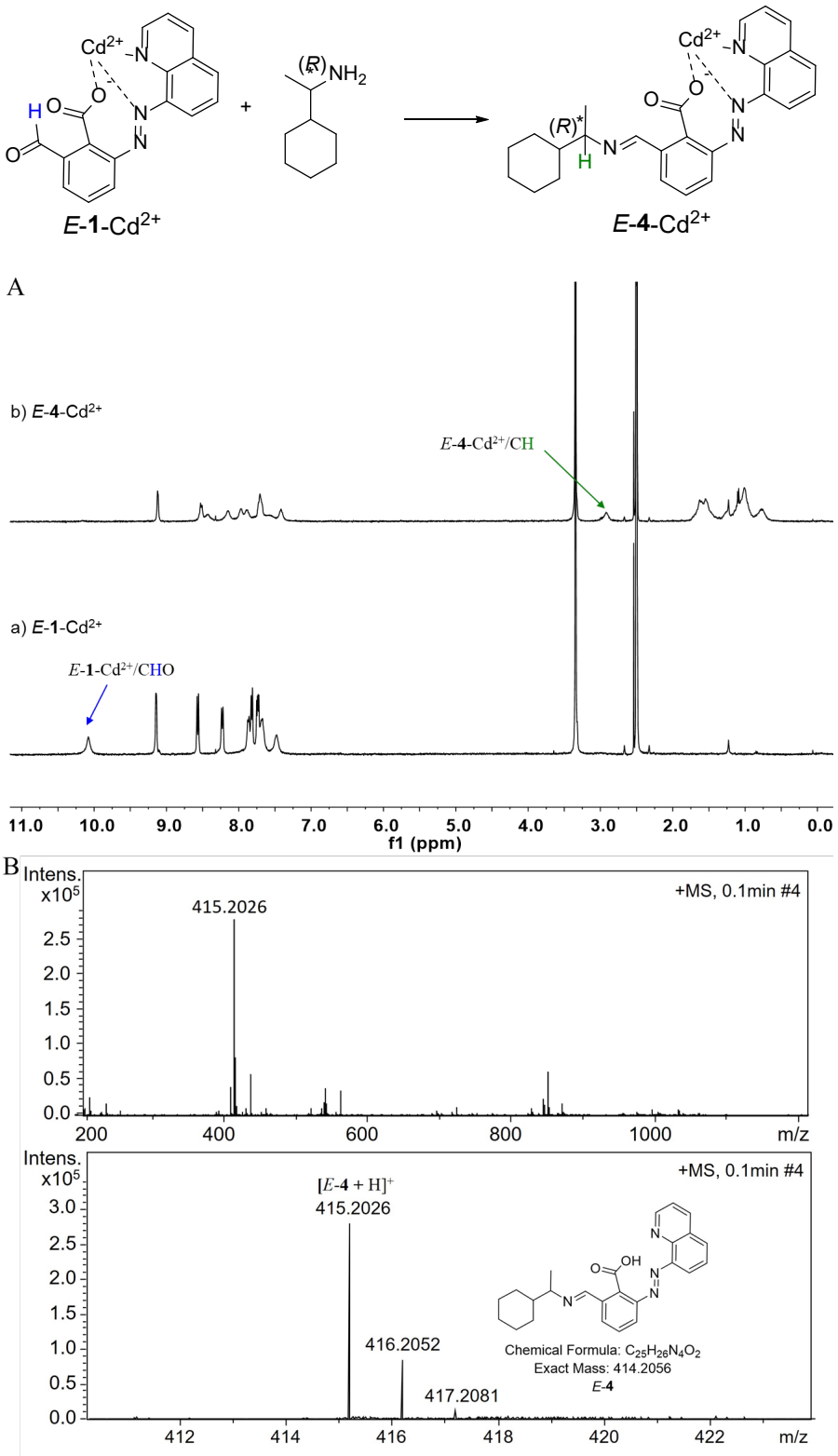

Figure S37. (A) ^{1}H NMR (400 MHz, 20 °C) spectrum of *E*-**1**-Cd^{2+} (10 mM) (a) and after addition of 1.5 equiv. of (*R*)-1-cyclohexylethylamine (b) in DMSO-d_6. The reaction reached equilibrium within 1.5 h. (B) MS spectra of *E*-**4**.

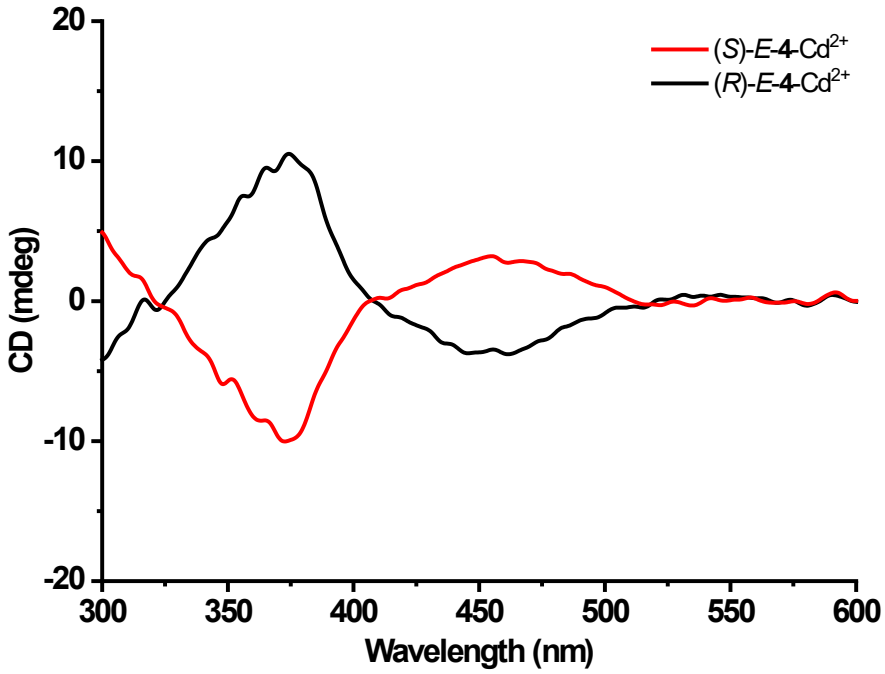

Figure S38. CD spectrum of *E*-**4**-Cd^{2+} (0.10 mM) in $CHCl_3$.

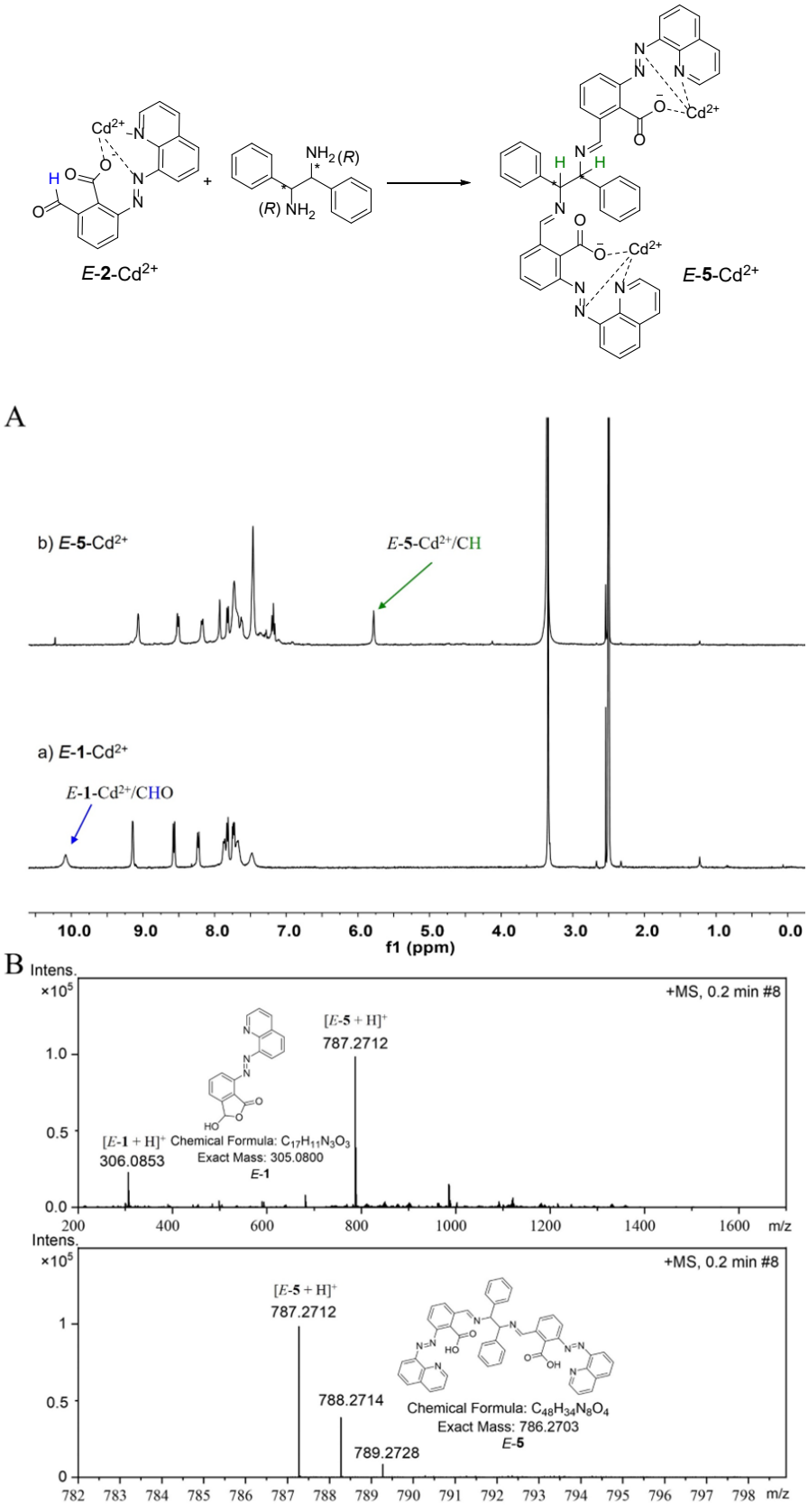

Figure S39. (A) ^{1}H NMR (400 MHz, 20 °C) spectrum of *E*-**1**-Cd^{2+} (10 mM) (a) and after addition of 0.45 equiv. of (1*R*,2*R*)-(+)-1,2-diphenylethylenediamine (b) in DMSO-d_6. The reaction reached equilibrium within 1.5 h. (B) MS spectra of *E*-**5**.

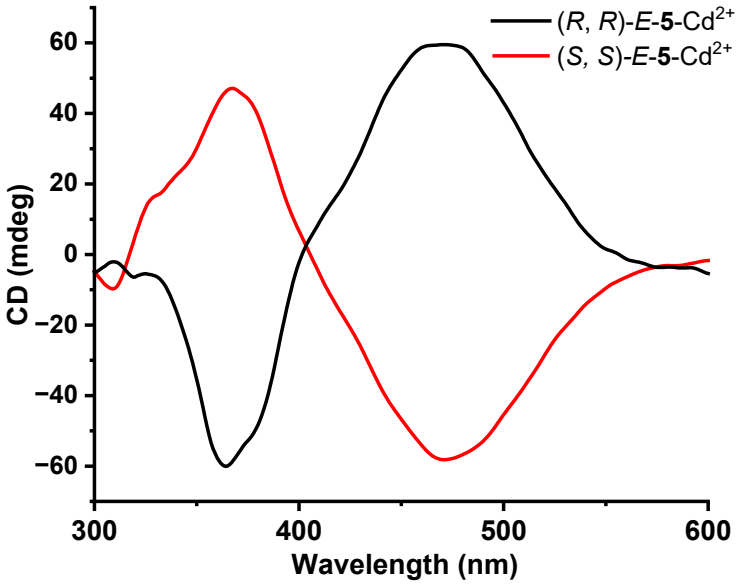

Figure S40. CD spectrum of *E*-**5**-Cd^{2+} (0.10 mM) in $CHCl_3$.

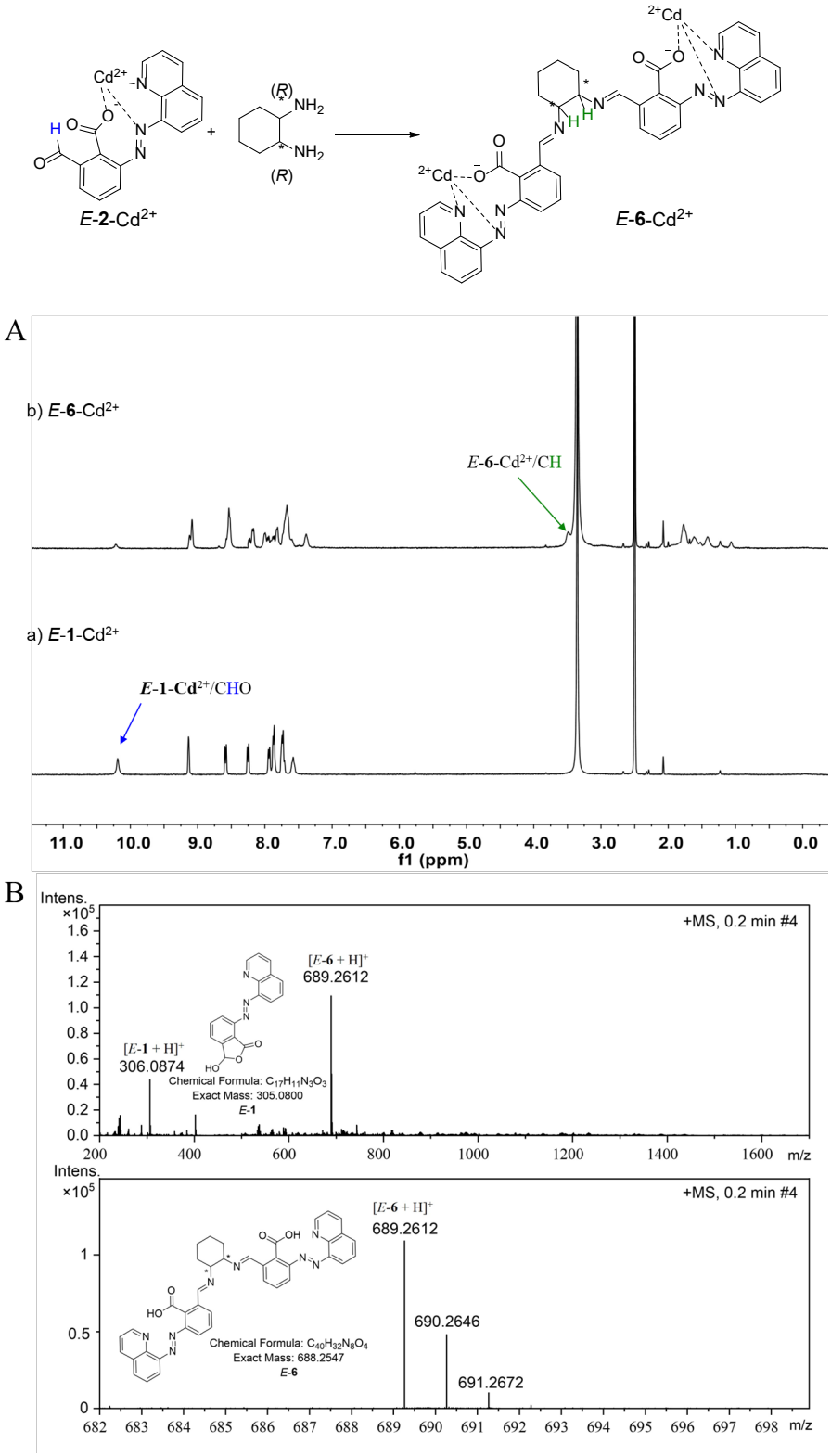

Figure S41. (A) ^{1}H NMR (400 MHz, 20 °C) spectrum of *E*-**1**-Cd^{2+} (10 mM) (a) and after addition of 0.45 equiv. of (1*R*,2*R*)-(-)-1,2-cyclohexanediamine (b) in DMSO-d_6. The reaction reached equilibrium within 1.5 h. (B) MS spectra of *E*-**6**.

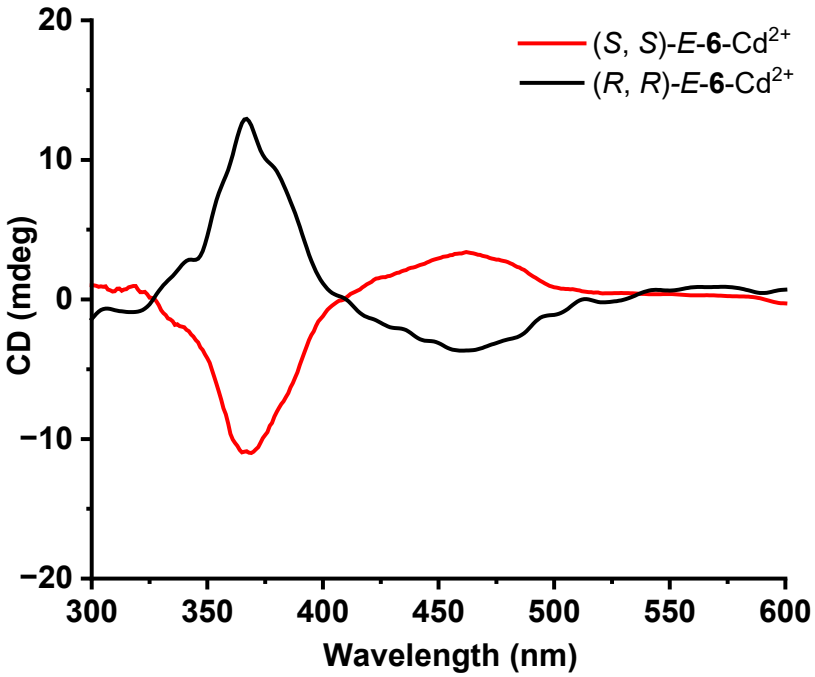

Figure S42. CD spectrum of *E*-**6**-Cd^{2+} (0.10 mM) in $CHCl_3$.

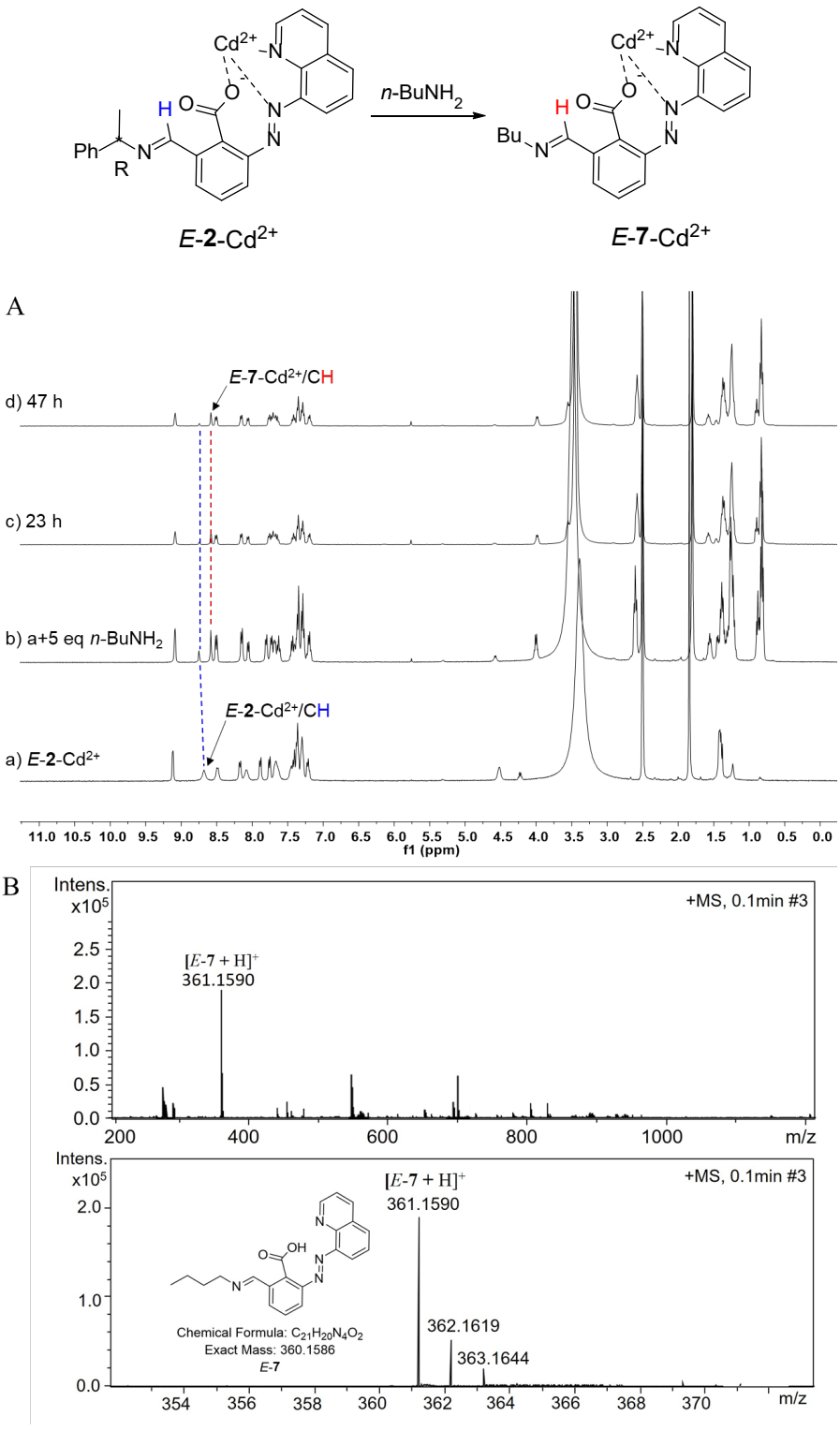

Figure S43. (A) ^{1}H NMR (400 MHz, 20 °C) spectra of (*R*)-*E*-**2**-Cd^{2+} (10 mM, a) and after addition of 5.0 equiv. of *n*-$BuNH_2$ (b) in DMSO-d_6. The reaction reached equilibrium within 24 h. (B) MS spectra of *E*-**7**.

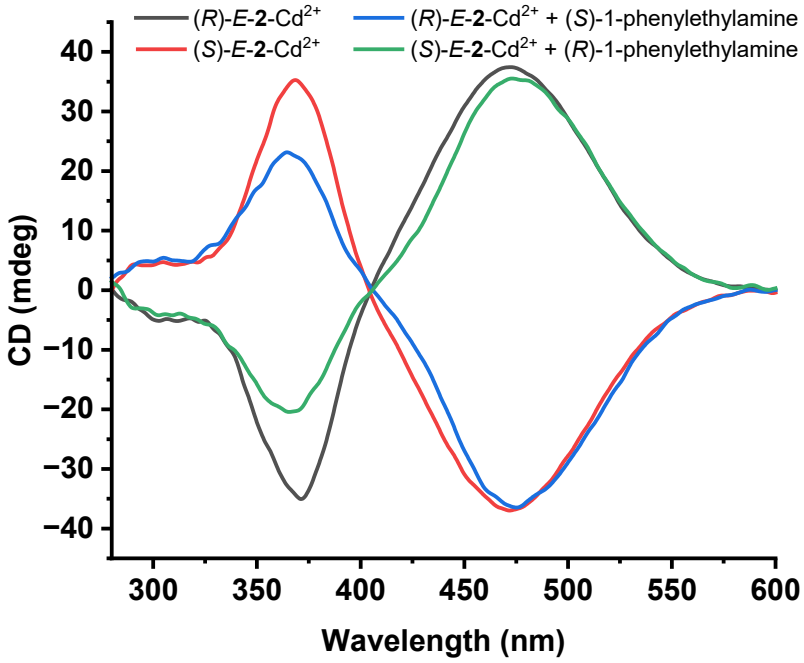

Figure S44. CD spectrum of DCRs of (*R*)/(*S*)-*E*-**2**-Cd^{2+} (0.10 mM) with 10 equiv. of (*S*)/(*R*)-1-phenylethylamine in $CHCl_3$.

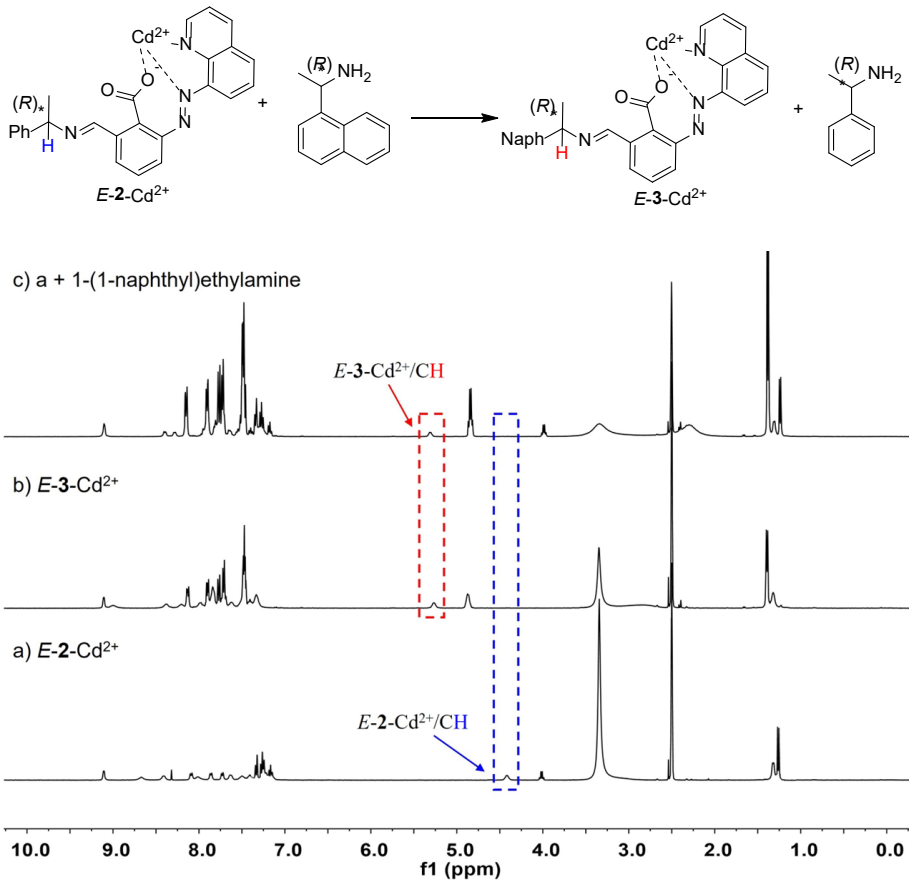

Figure S45. ^{1}H NMR (400 MHz, 20 °C) spectra of *E*-**2**-Cd^{2+} (10 mM) (a) and *E*-**3**-Cd^{2+} (10 mM) in DMSO-d_6 (b). After addition of 10.0 equiv. of (*R*)-1-(1-naphthyl)ethylamine into panel a to create *E*-**3**-Cd^{2+} (c). The reaction reached equilibrium within 24 h.

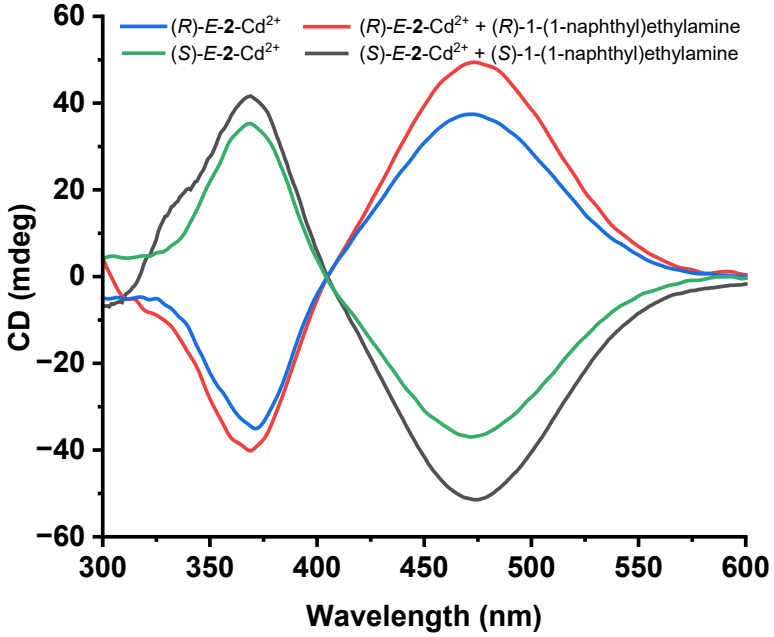

Figure S46. CD spectrum of DCRs of (*R*)/(*S*)-*E*-**2**-Cd^{2+} (0.10 mM) with 10.0 equiv. of (*R*)/(*S*)-1-(1-naphthyl)ethylamine in $CHCl_3$.

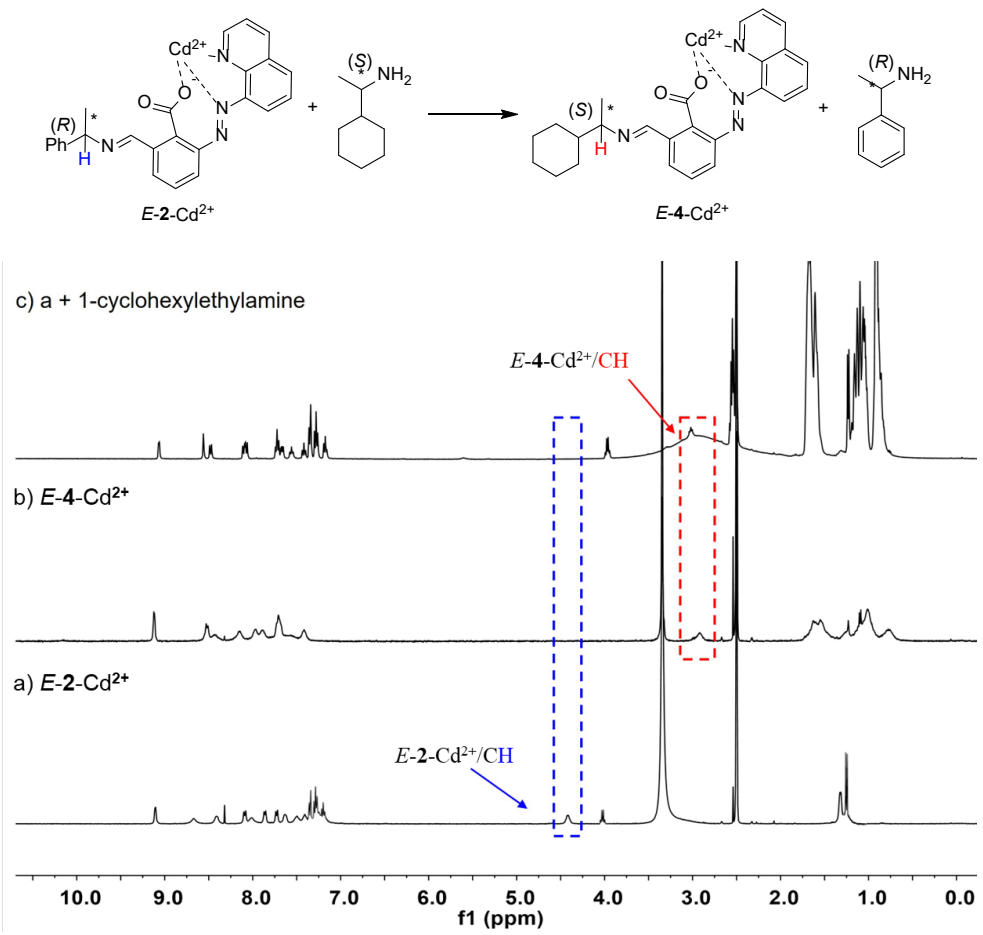

Figure S47. ^{1}H NMR (400 MHz, 20 °C) spectra of *E*-**2**-Cd^{2+} (10 mM) (a) and *E*-**4**-Cd^{2+} (10 mM) in DMSO-d_6 (b). After addition of 10.0 equiv. of (*S*)-1-cyclohexylethylamine into panel a to create *E*-**4**-Cd^{2+} (c). The reaction reached equilibrium within 24 h.

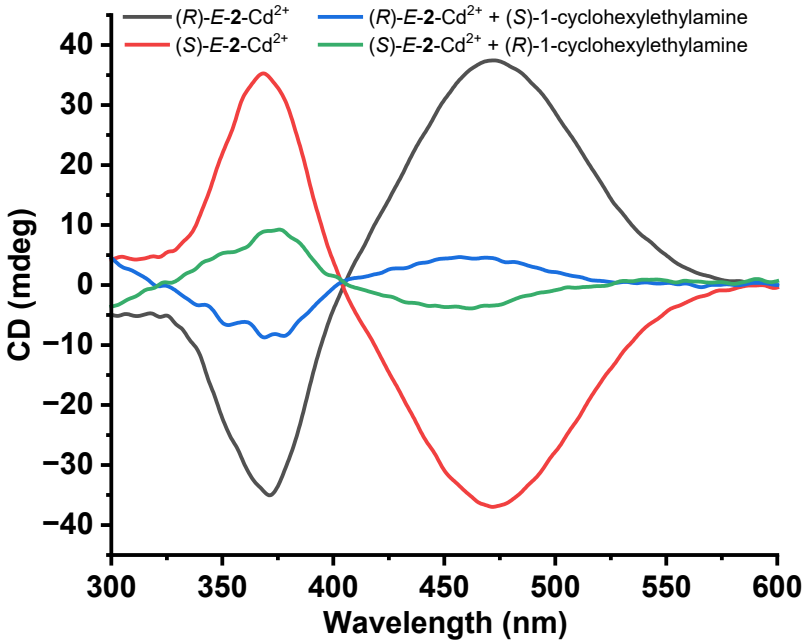

Figure S48. CD spectrum of DCRs of (*R*)/(*S*)-*E*-**2**-Cd^{2+} (0.10 mM) with 10.0 equiv. of (*S*)/(*R*)-1-cyclohexylethylamine in $CHCl_3$.

6. Molecular coordinate

(*M, S*)-*E*-**2** (DMSO)

Imaginary frequency: 0

G = -1332.4280070 hartree

O	0.28488900	-1.56012700	0.47072800
O	0.51242300	-0.51829000	-1.51621200
N	2.73321300	0.66773800	0.08448000
N	2.21210900	1.80719600	0.06113200
N	4.35853700	-1.39997400	0.91026200
C	-0.05664800	0.78791400	0.35982100
C	4.85210600	-0.51780000	0.00158200
C	-1.38502900	1.02459700	0.78458600
C	0.85678200	1.87209600	0.43663000
C	0.30947300	-0.56374300	-0.28543400
C	4.04313200	0.59223200	-0.42164700
C	0.44212800	3.13788800	0.88411300
H	1.18467000	3.93830500	0.90661600
C	6.17217200	-0.64712100	-0.54599800
C	4.54297900	1.49897600	-1.34962800
H	3.89596200	2.31725600	-1.66744800
C	-0.87083600	3.35156200	1.30074400
H	-1.18396700	4.33385400	1.66088600
C	5.12082500	-2.40472900	1.28898800
H	4.69115200	-3.10354300	2.01744100
C	-1.77627800	2.29474900	1.24878900
H	-2.81403300	2.42710600	1.55931400
C	5.84066200	1.35583300	-1.88229600
H	6.20372200	2.08019800	-2.61480200
C	6.43878400	-2.62601600	0.81253700
H	7.01302600	-3.48113200	1.17373100
C	6.96065600	-1.74386400	-0.10595100
H	7.97073500	-1.87002500	-0.50367900
C	-2.38731600	-0.06207100	0.73508500
H	-1.98708200	-1.06819700	0.52180100
C	6.64526500	0.30427000	-1.48858500
H	7.65095200	0.18571700	-1.89885900
N	-3.62888900	0.13747700	0.94413200
C	-4.52242100	-1.00698800	0.89228100
H	-3.97088500	-1.92455800	0.60334800
C	-5.62244900	-0.78374200	-0.13595800
C	-6.15083500	0.49422600	-0.37093400
C	-6.15800900	-1.87392100	-0.83635900
C	-7.19451500	0.67583100	-1.28283800
H	-5.72658600	1.34677500	0.16138700
C	-7.20332500	-1.69549400	-1.74764100
H	-5.74902700	-2.87428300	-0.66798700
C	-7.72597600	-0.41819300	-1.97389900
H	-7.59361300	1.67845300	-1.45724800
H	-7.60654600	-2.55627300	-2.28707700
H	-8.54012000	-0.27543300	-2.68868800
C	-5.12440900	-1.23628800	2.28818700
H	-5.81656100	-2.09167000	2.27323500
H	-5.67938800	-0.34330800	2.61492600
H	-4.32721300	-1.44019500	3.01988000

(*P, S*)-*E*-**2** (DMSO)

Imaginary frequency: 0

G = -1332.4278440 hartree

O	4.54354100	8.68942000	6.73044700
O	4.95226300	10.11434200	8.42868100
N	6.85895000	11.11376400	6.37150900
N	6.24342800	12.20483300	6.36313700
N	8.62401700	9.20868000	5.43663600
C	4.05116900	11.00251200	6.44409300
C	9.09261200	10.15637900	6.29111500
C	2.67771700	11.07066200	6.11258300
C	4.85833400	12.12403100	6.11885900
C	4.59183700	9.81692700	7.27091700
C	8.20751300	11.18516700	6.76304000
C	4.30137800	13.27505000	5.53889100
H	4.96689300	14.11518700	5.32958100
C	10.45827500	10.17888300	6.73044000
C	8.67855700	12.15910100	7.63562400
H	7.97465900	12.91022800	7.99569200
C	2.94338100	13.32694000	5.22593800
H	2.51666100	14.21974800	4.76385700
C	9.45695100	8.28319100	5.00761000
H	9.04758400	7.52787500	4.32537100
C	2.14084000	12.22584400	5.51196500
H	1.07275100	12.23524600	5.28816700
C	10.02202000	12.16298200	8.06520900
H	10.36216200	12.93577300	8.75811500
C	10.82539600	8.21367600	5.37550000
H	11.45747500	7.41813800	4.97674600
C	11.32197500	9.16394400	6.23856600

H	12.36879000	9.15367400	6.55234500
C	1.78285500	9.92800800	6.39868400
H	2.28555000	9.01049800	6.74833200
C	10.90014900	11.19404000	7.62070300
H	11.94178200	11.19032600	7.95042300
N	0.52028700	9.98293200	6.22952500
C	-0.25899400	8.79536400	6.53933500
H	0.40170400	7.96047900	6.84860000
C	-1.04479600	8.33779400	5.31922300
C	-1.23131900	6.97011200	5.07534900
C	-1.63118100	9.26533700	4.44488700
C	-1.99227700	6.53452200	3.98580200
H	-0.77276800	6.23753900	5.74558600
C	-2.39010100	8.83306100	3.35399600
H	-1.47761500	10.33084100	4.62349000
C	-2.57479100	7.46577400	3.12070800
H	-2.12525900	5.46413200	3.80942700
H	-2.83845400	9.56756100	2.67992400
H	-3.16644500	7.12812300	2.26627100
C	-1.20534300	9.10853300	7.70931400
H	-0.62809000	9.39881700	8.60096000
H	-1.87896700	9.93797200	7.44396300
H	-1.81665800	8.22743800	7.95636600

(*P, S*)-*E*-**2**-Cd^{2+} (DMSO)

Imaginary frequency: 0

G = -2832.5489400 hartree

Cd	-0.00055200	0.41468600	-0.00091400
O	-1.59005600	-0.08153900	-3.70596000
O	-1.23928600	0.98032800	-1.76453800
O	1.23968100	0.98212100	1.76113500
O	1.59096800	-0.07635500	3.70431500
N	0.27883400	-1.70108800	-1.61022100
N	-0.27847600	-1.69901000	1.61246000
N	0.52411700	-2.65517600	1.73119900
N	-0.52396700	-2.65695200	-1.72975900
N	-2.10414000	0.30916800	1.17446100
N	2.10399300	0.30816500	-1.17496700
C	-2.45085500	-1.08950300	-1.75383200
C	2.45122300	-1.08773600	1.75370700
C	-1.87109600	-2.35362600	-1.47794800
C	-2.52342500	-0.83143800	1.78506400
C	2.94338700	1.31897100	-1.02909800
H	2.56092100	2.20302300	-0.51309200
C	3.87612700	-0.97707800	-2.23093100
C	3.82023600	-0.90910500	1.47577600
C	2.52353700	-0.83300900	-1.78426900
C	-1.67824000	0.01302200	-2.48437600
C	1.87122300	-2.35207100	1.47922000
C	1.67877900	0.01607200	2.48253300
C	-1.61289900	-1.92151400	1.98719100
C	2.64523400	-3.40030300	0.95424600
H	2.15841900	-4.35935500	0.77026700
C	-3.87595300	-0.97527900	2.23194600
C	1.61323000	-1.92348600	-1.98526800
C	-2.06065400	-3.09867400	2.57477500
H	-1.34320600	-3.90577600	2.72286100
C	-3.81975700	-0.91014000	-1.47573500
C	3.98715300	-3.19406700	0.64479000
H	4.57782200	-3.99736200	0.20176100
C	-2.94360100	1.31985200	1.02805200
H	-2.56134200	2.20350600	0.51119100
C	4.56837400	-1.95551200	0.90809800
H	5.62187600	-1.77143600	0.69446900
C	4.74848100	0.12950900	-2.06380900
H	5.78632300	0.05114700	-2.39407100
C	2.06110900	-3.10100000	-2.57203600
H	1.34381300	-3.90837700	-2.71933800
C	-3.40171900	-3.24131600	2.97714400
H	-3.72977700	-4.17937800	3.42870900
C	-4.28006300	1.28640300	1.48066900
H	-4.92153600	2.15395500	1.33729400
C	-4.74837600	0.13115500	2.06418800
H	-5.78614900	0.05300200	2.39471200
C	3.40213700	-3.24370300	-2.97449500
H	3.73028900	-4.18203600	-3.42542200
C	4.28003000	1.28514700	-1.48116400
H	4.92149000	2.15278200	-1.33816800
C	4.29426300	-2.20004900	-2.81621000
H	5.33247400	-2.29944100	-3.13969400
C	-4.47724600	0.37421700	-1.79194100
H	-3.81191700	1.19730400	-2.10935900
C	-2.64527800	-3.40118800	-0.95194700
H	-2.15870100	-4.36016500	-0.76695300
C	-3.98715300	-3.19432000	-0.64270000
H	-4.57801000	-3.99706400	-0.19892000
C	4.47816200	0.37513000	1.79149000
H	3.81312700	1.19860100	2.10853800

C	-4.29396200	-2.19788000	2.81810600
H	-5.33216100	-2.29714800	3.14166800
C	-4.56809300	-1.95584900	-0.90705600
H	-5.62151500	-1.77132900	-0.69343000
N	-5.73454200	0.53931000	-1.69093400
C	-6.28162900	1.85965000	-1.97312500
H	-5.50179400	2.52498400	-2.39308100
C	-7.41618000	1.73594300	-2.99625900
H	-8.21697000	1.08758600	-2.60899900
H	-7.84331300	2.72592500	-3.21623300
H	-7.03925700	1.29922800	-3.93407700
C	-6.75513400	2.47619600	-0.66563900
C	-6.36438000	3.77282000	-0.30873500
C	-7.56117800	1.74324200	0.21929300
C	-6.76430900	4.32884800	0.91173100
H	-5.72720300	4.34793900	-0.98572800
C	-7.95853900	2.29370600	1.43941500
H	-7.85384600	0.72495800	-0.04287600
C	-7.55849200	3.58841900	1.79184300
H	-6.44523200	5.33923600	1.17862500
H	-8.57734400	1.70785800	2.12361900
H	-7.86355600	4.01624200	2.74968900
N	5.73556600	0.53961300	1.69086700
C	6.28311000	1.85979700	1.97305400
H	5.50376500	2.52499300	2.39412100
C	6.75518100	2.47685800	0.66530800
C	6.36307700	3.77317600	0.30880700
C	7.56117000	1.74463600	-0.22029400
C	6.76168400	4.32967200	-0.91188100
H	5.72594100	4.34770300	0.98634100
C	7.95720500	2.29555900	-1.44063500
H	7.85489800	0.72656800	0.04154500
C	7.55585900	3.58999700	-1.79262300
H	6.44160900	5.33983800	-1.17841800
H	8.57600700	1.71030500	-2.12534900
H	7.85992900	4.01819300	-2.75061900
C	7.41868000	1.73546100	2.99495900
H	7.04269500	1.29813500	3.93286900
H	8.21906900	1.08731900	2.60651100
H	7.84606600	2.72528300	3.21516500

(*M, S*)-*E*-**2**-Cd^{2+} (DMSO)

Imaginary frequency: 0

G = -2832.5383040 hartree

Cd	0.05678100	-0.04415000	-0.56505700
O	3.16806200	-2.64184100	0.27363200
O	1.86292000	-1.28561400	-0.93516000
O	-1.75859900	0.94607000	-1.37557700
O	-2.83799800	2.78057700	-0.67567000
N	0.51388900	-1.16204500	1.80557700
N	-0.41322900	1.85515700	1.23994900
N	-1.23171400	1.80479900	2.18907900
N	1.34150700	-0.79376000	2.67340000
N	1.49575100	1.88966600	-0.74425900
N	-1.39632900	-1.91968900	-0.02951000
C	3.07469400	-0.38792100	0.94109600
C	-2.97153800	0.86099900	0.69142800
C	2.47939100	-0.12621800	2.19863200
C	1.61830500	2.75905200	0.29500600
C	-2.26621900	-2.32062900	-0.93961500
H	-2.13798800	-1.92079300	-1.94890700
C	-2.59427400	-3.20993600	1.64678300
C	-4.13319000	0.06966300	0.59503100
C	-1.51789400	-2.35120000	1.25476400
C	2.64952000	-1.55083500	0.03990000
C	-2.37798700	1.02771500	1.96704200
C	-2.47077500	1.61629600	-0.54336300
C	0.67269000	2.73691700	1.37355200
C	-2.94757200	0.43854400	3.10884000
H	-2.46476800	0.60774600	4.07248800
C	2.69138900	3.70515300	0.34239200
C	-0.56875900	-1.94220500	2.24931600
C	0.83318100	3.59895700	2.45195100
H	0.09509800	3.56379800	3.25314100
C	4.22347700	0.34527900	0.58367200
C	-4.07629900	-0.36775000	2.99198500
H	-4.49673600	-0.85424400	3.87343800
C	2.35598800	1.93946200	-1.74591100
H	2.22244500	1.20340000	-2.54306600
C	-4.66457000	-0.54675300	1.74113700
H	-5.55891800	-1.15979300	1.62302800
C	-3.50538400	-3.62844300	0.64300400
H	-4.33534600	-4.28411200	0.91503400
C	-0.72669500	-2.35407600	3.56744800
H	0.01324200	-2.03100200	4.29946600
C	1.91241100	4.50058900	2.50367300
H	2.01930200	5.16083900	3.36628400
C	3.42156400	2.86383900	-1.80276100

H	4.09577800	2.85790500	-2.65915500
C	3.59544500	3.73483600	-0.75091800
H	4.42317200	4.44718800	-0.73973200
C	-1.80668500	-3.17264900	3.94625400
H	-1.91071500	-3.47526300	4.98983100
C	-3.33498900	-3.19717300	-0.65283000
H	-4.01464400	-3.49825500	-1.44925100
C	-2.72141600	-3.60237700	3.00375800
H	-3.55488400	-4.24781800	3.28809000
C	4.88440100	0.06937300	-0.70660600
H	4.28079300	-0.48811200	-1.44536800
C	3.03975700	0.81972300	3.07546400
H	2.55611300	0.97697100	4.04071300
C	4.15972700	1.55360200	2.69578700
H	4.57206100	2.31054700	3.36468800
C	-4.81114900	-0.08945600	-0.70848800
H	-4.26829900	0.29738300	-1.58985100
C	2.82182600	4.56246200	1.46499100
H	3.65378100	5.26908900	1.49277800
C	4.74850800	1.31330500	1.45489200
H	5.63604000	1.86175500	1.13625200
N	6.07540200	0.43536200	-0.96484000
C	6.62929800	0.06598700	-2.26327400
H	5.82518600	-0.32141900	-2.92276900
C	7.22934100	1.30671900	-2.91856000
H	8.02695600	1.73526000	-2.29330100
H	6.44981400	2.07207600	-3.04433000
H	7.64268900	1.07337600	-3.91071200
C	7.61394700	-1.08724100	-2.05309900
C	8.96687400	-1.00687700	-2.40643500
C	7.13978300	-2.28407900	-1.48820900
C	9.82530600	-2.09498800	-2.20601300
H	9.36734800	-0.09293700	-2.84624700
C	7.99205100	-3.37079300	-1.28923400
H	6.09047300	-2.36724100	-1.19337400
C	9.34235800	-3.28002500	-1.64800200
H	10.87749800	-2.01115900	-2.48918700
H	7.60202000	-4.29294700	-0.85132700
H	10.01202800	-4.12913100	-1.49179700
N	-5.95410200	-0.63584600	-0.82288200
C	-6.54952700	-0.72258600	-2.14665300
H	-5.86929000	-0.29867100	-2.91212700
C	-7.84685000	0.07305300	-2.18801600
C	-8.72566800	0.08463100	-1.09443500
C	-8.20126600	0.77629900	-3.34742100
C	-9.93486100	0.78174100	-1.16254100
H	-8.44771500	-0.44920800	-0.18420300
C	-9.41195200	1.47253600	-3.41884200
H	-7.52027700	0.78072500	-4.20309200
C	-10.28339600	1.47733100	-2.32545200
H	-10.60835900	0.78443700	-0.30166500
H	-9.67192100	2.01764700	-4.32967900
H	-11.22796300	2.02423700	-2.37733100
C	-6.80376600	-2.19639100	-2.49479800
H	-7.28881400	-2.27782900	-3.47881200
H	-7.45884700	-2.65999600	-1.74149200
H	-5.85643900	-2.75502600	-2.52700000

(*M, S*)-*Z*-**2**-Cd^{2+} (DMSO)

Imaginary frequency: 0

G = -1667.582640 hartree

O	1.50798300	-0.12700500	-2.57579100
O	0.39687900	-1.82165800	-1.67131700
N	-2.37165300	-0.10323700	-0.00616800
N	-1.24530000	-0.59611100	0.22311600
N	-4.93964700	0.76704700	0.43146900
C	1.08211300	0.02038500	-0.25552500
C	-4.01448900	1.66192800	-0.00681100
C	2.25820900	0.67724600	0.17352500
C	-0.08000600	0.17162600	0.52577000
C	1.00861500	-0.68818600	-1.60558000
C	-2.65539800	1.25368800	-0.24624500
C	-0.10120500	0.95355500	1.68933600
H	-1.02073300	1.04154800	2.26961600
C	-4.37603300	3.02496100	-0.23781900
C	-1.75452900	2.16355200	-0.80076600
H	-0.74444200	1.85295700	-1.05512900
C	1.06980000	1.58543700	2.09931000
H	1.07023000	2.18417900	3.01202200
C	-6.18065900	1.15711900	0.68875600
H	-6.88173400	0.38719800	1.01846400
C	2.23699700	1.44145400	1.35168500
H	3.16529600	1.92096700	1.66343500
C	-2.13849100	3.48874400	-1.06755200
H	-1.41051500	4.17289400	-1.50511200
C	-6.60425500	2.49306400	0.54094400
H	-7.63255100	2.76199400	0.78289200
C	-5.70475400	3.42141300	0.06447200

H	-5.99852300	4.46144800	-0.09082400
C	3.53264100	0.54818900	-0.57361700
H	3.54138600	-0.15038600	-1.42446900
C	-3.41377200	3.92502600	-0.76344900
H	-3.70276800	4.96358600	-0.93555700
N	4.56681800	1.20901000	-0.24008200
C	5.78839100	1.00897100	-1.00430800
H	5.63603200	0.25046400	-1.79740900
C	6.89723400	0.51020000	-0.08954700
C	7.77147700	-0.49383300	-0.52647000
C	7.08785500	1.06673300	1.18451500
C	8.82164700	-0.93084800	0.28760300
H	7.62779900	-0.93920900	-1.51478800
C	8.13398300	0.62958700	2.00083400
H	6.40329000	1.84109300	1.53532800
C	9.00583400	-0.37017800	1.55481000
H	9.49437200	-1.71510600	-0.06832000
H	8.26951200	1.07028300	2.99180300
H	9.82319700	-0.71244900	2.19412500
C	6.17854100	2.33377100	-1.67666100
H	5.38189000	2.66634000	-2.36000900
H	6.33876400	3.11581500	-0.91884200
H	7.10773300	2.20888100	-2.25242900
Cd	-4.31852500	-1.46420900	0.32380500
Cd	-0.61641500	-2.93270300	-0.12108800

(*P, S*)-*Z*-**2**-Cd^{2+} (DMSO)

Imaginary frequency: 0

G = -1667.581920 hartree

O	1.70432300	-0.88039900	2.10523300
O	0.25089100	-2.39113200	1.37415600
N	-2.31774500	0.00750600	0.10127000
N	-1.39954900	-0.75913800	-0.25852800
N	-4.59066200	1.53179100	-0.14471100
C	1.05267500	-0.70647400	-0.16109000
C	-3.41584300	2.15533300	0.14166100
C	2.26980100	-0.35012400	-0.78523700
C	-0.14720700	-0.30554000	-0.77766100
C	1.01735100	-1.36802900	1.21267000
C	-2.20186200	1.39973100	0.28103700
C	-0.16468100	0.42240100	-1.97524700
H	-1.11665300	0.71000800	-2.42395200
C	-3.36726200	3.57445200	0.30256900
C	-1.03488700	2.04535500	0.68883100
H	-0.12664800	1.47687400	0.87308800
C	1.04436400	0.74236700	-2.58826700
H	1.04387200	1.29254800	-3.53104300
C	-5.69820400	2.24108000	-0.32251500
H	-6.61387800	1.68338200	-0.53037900
C	2.24650800	0.35498300	-2.00015600
H	3.20225000	0.59346100	-2.46770400
C	-1.01439500	3.43540500	0.89635100
H	-0.08631200	3.90888700	1.21886200
C	-5.72329800	3.64746700	-0.24146200
H	-6.65837600	4.17988500	-0.41574300
C	-4.56097000	4.31046300	0.08626900
H	-4.54201800	5.39741400	0.18803700
C	3.57785700	-0.72375600	-0.19572300
H	3.55211300	-1.28661400	0.75033400
C	-2.14704800	4.19468500	0.67456800
H	-2.12338100	5.27931400	0.79495100
N	4.67451700	-0.40090300	-0.75337300
C	5.91737900	-0.81621700	-0.12280500
H	5.71892600	-1.31768200	0.84502200
C	6.79507800	0.39666900	0.14840900
C	6.92867100	1.41829300	-0.80428800
C	7.51821500	0.48934600	1.34493500
C	7.77272000	2.50566500	-0.56573100
H	6.35792700	1.35868600	-1.73266900
C	8.36581500	1.57585500	1.58513100
H	7.41593700	-0.29715400	2.09779700
C	8.49567700	2.58794200	0.62965700
H	7.86583300	3.29495100	-1.31607000
H	8.92206500	1.63343800	2.52404300
H	9.15457700	3.43938700	0.81637400
C	6.63177500	-1.81957700	-1.04148600
H	7.58382500	-2.13612700	-0.58997000
H	6.84377100	-1.36138000	-2.01954700
H	6.00325800	-2.70959400	-1.19998600
Cd	-4.64101800	-0.75230400	0.08367900
Cd	-1.26636000	-3.20746400	0.06649400

7. References

S1. C. E. Weston, R. D. Richardson, P. R. Haycock, A. J. P. White and M. J. Fuchter, Arylazopyrazoles: Azoheteroarene Photoswitches Offering Quantitative Isomerization and Long Thermal Half-lives, *J. Am. Chem. Soc.,* 2014, **136**, 11878–11881.

S2. M. J. Frisch, G. W. Trucks, H. B. Schlegel, G. E. Scuseria, M. A. Robb, J. R. Cheeseman, G. Scalmani, V. Barone, B. Mennucci, G. A. Petersson, H. Nakatsuji, M. Caricato, X. Li, H. P. Hratchian, A. F. Izmaylov, J. Bloino, G. Zheng, J. L. Sonnenberg, M. Hada, M. Ehara, K. Toyota, R. Fukuda, J. Hasegawa, M. Ishida, T. Nakajima, Y. Honda, O. Kitao, H. Nakai, T. Vreven, J. A. Jr. Montgomery, J. E. Peralta, F. Ogliaro, M. Bearpark, J. J. Heyd, E. Brothers, K. N. Kudin, V. N. Staroverov, R. Kobayashi, J. Normand, K. Raghavachari, A. Rendell, J. C. Burant, S. S. Iyengar, J. Tomasi, M. Cossi, N. Rega, J. M. Millam, M. Klene, J. E. Knox, J. B. Cross, V. Bakken, C. Adamo, J. Jaramillo, R. Gomperts, R. E. Stratmann, O. Yazyev, A. J. Austin, R. Cammi, C. Pomelli, J. W. Ochterski, R. L. Martin, K. Morokuma, V. G. Zakrzewski, G. A. Voth, P. Salvador, J. J. Dannenberg, S. Dapprich, A. D. Daniels, Ö. Farkas, J. B. Foresman, J. V. Ortiz, J. Cioslowski, D. J. Fox, Gaussian 09, Revision D.01, Gaussian, Inc., Wallingford, CT, **2010**.

S3. T. Lu, F. Chen, Multiwfn: A Multifunctional Wavefunction Analyzer, *J. Comput. Chem.,* 2012, **33**, 580-592.

S4. W. Humphrey, A. Dalke, K. Schulten, VMD: Visual Molecular Dynamics, *J. Mol. Graphics,* 1996, **14**, 33-38.

S5. Y. Lv, H. Ye and L. You, Multiple Control of Azoquinoline Based Molecular Photoswitches, *Chem. Sci.,* 2024, **15**, 3290–3299.